Self-Healing of Thermoplastic Poly(Ethylene-co-Methacrylic Acid) Copolymers Following Projectile Puncture

by

Stephen James Kalista, Jr.

Thesis submitted to the faculty of
Virginia Polytechnic Institute and State University
in partial fulfillment of the requirements for the degree of

MASTER OF SCIENCE

In

Engineering Mechanics

Thomas C. Ward, Chairman
John J. Lesko, Chairman
Brian J. Love

September 1, 2003
Blacksburg, Virginia

Keywords: self-healing, puncture reversal, ionomer, thermoplastic, EMAA, multi-wall carbon nanotube

Self-Healing of Thermoplastic Poly(Ethylene-co-Methacrylic Acid) Copolymers Following Projectile Puncture

Stephen James Kalista, Jr.

(ABSTRACT)

Poly(ethylene-co-methacrylic acid) (EMAA) ionomer polymers carry great potential for use in a wide variety of unique applications due to their property of "self-healing" following projectile impact. Following puncture, certain films based on these materials are observed to "heal", with the penetration opening recovering to an air-tight condition. Specifically, four polymers of this class were examined, including DuPont™ Surlyn® 8920, Surlyn® 8940, Nucrel® 925, and Nucrel® 960. Though these differ in their amount of ionic content, all expressed a certain degree of self-healing. Thin films were prepared by a compression molding process and punctured at temperatures ranging from room up to that of the melt using a pellet gun. Samples were then assessed for self-healing. A quantitative post-puncture burst-test method examined the strength or quality of the healed site in the four examples. A comparison of this data provided an understanding of the importance of ionic content and the mechanism of puncture healing. Additional damage modes were also examined to determine other cases where healing occurs and the requirements necessary to elicit the healing response. In addition, interesting composite materials consisting of carbon nanotube filled ionomers were fabricated by a melt-mixing process which produced potentially self-healing composites with superior mechanical properties. By comparing peel testing, projectile testing, the quantitative healed strength, and other characteristics, it was determined that healing is not a function of the ionic content of the materials involved. Further, healing was determined to occur due to a synergy of thermomechanical properties facilitated by the addition of the methacrylic acid groups to the polymer backbone.

Acknowledgements

Many individuals have contributed to making this project happen and I would like to express my sincerest gratitude for their help over the last two years.

I would first like to thank some of those who helped with setup and testing. Zainab Oyetunji, an undergraduate SURP student from U. Maine, spent a summer working with me on this project performing experiments. The Physics Machine Shop gave many hours going over drawings and fabricating many of the test fixtures used in the project. Dr. Mia Siochi at NASA LaRC provided many ideas through her coordinated research and correspondence. DuPont donated materials used in this project.

I would like to thank the members of the PolyPKem Research Group and Dr. Taigyoo Park for their many contributions. Not only did they provide me with help on experiments, design, and analysis but they have been great friends and colleagues through it all. Thank you all for the great conversations and the enriching experiences day-in, day-out in the lab. Also, I would like to thank my advisor, Dr. Ward. From you, I have not only learned much about research but I have learned much about life. You serve as a model of what an educator should be and I hope someday to do as much.

Finally, I would like to thank a most wonderful group who made all of this so very special. I know that without them, at times things would have simply seemed unattainable. I want to thank my parents for their constant support and love. Not only have they provided me with encouragement in getting through this, but they have lovingly motivated me to learn and accomplish so much. I would like to thank my friends including Selanga, Mark and Aaron for all the moral support. You all were always there to help give a hand or lend an ear, whenever necessary. And last but not least, I would like to thank Anne. You have shown me love and support through it all—encouraging me to pursue my dreams and inspiring me to learn and grow. Even when I felt lost or overwhelmed, you always assured me that no matter what, things always seem to work out.

I thank all of you. I want everyone to know, you have made this experience special and I love you all.

TABLE OF CONTENTS

LIST OF FIGURES

LIST OF TABLES

1. Introduction

A certain class of poly(ethylene-co-methacrylic acid) (EMAA) materials has been observed to exhibit a unique self-healing behavior upon projectile puncture.[1] This self-healing behavior occurs as an automatic response to puncture without manual intervention. Though ionomers have existed since the 1960's, the self-healing behavior expressed by these polymers has only recently been studied. This phenomenon holds exciting potential for use in a wide variety of unique applications. However, to effectively utilize the self-healing behavior and to produce novel materials which possess this response, the mechanism by which they heal must first be understood.

Characteristically, the self-healing response is noted following projectile penetration and originates from some puncture reversal mechanism. However, the actual healing process has not been observed visually since it occurs quite rapidly (fractions of a second). It has been hypothesized that the self-healing response is related to the ionic groups present in these copolymers.[1] This ionic content is known to have drastic effects on bulk mechanical properties. During puncture, energy is known to be transferred to these materials heating them to the melt state. After penetration, one proposition is that these ionomers maintain their ionic attractions, driving flow of the melt material which leads to patching of the hole.

In order to test this hypothesis and determine the effect of the ionic groups, EMAA materials of varying ionic content were examined. These include two of the ion-containing ionomers with differing levels of ionic content as well as the base copolymers from which they are formed which contain no ionic groups. Each sample's ability in self-healing was assessed and compared.

A number of techniques were employed to clarify the reason for the self-healing behavior and the mechanics involved. These included traditional characterization techniques such as DSC, TGA and SEM, as well as more mechanical methods involving peel testing,

controlled projectile testing, and a novel quantitative pressurized burst test. By comparing the results for each material tested, the role of ionic content could be revealed. Beyond projectile testing, several other damage modes were examined for the possible healing response. This revealed much information on the criteria necessary for healing to occur. Additionally, carbon nanotube filled EMAA ionomers were fabricated and also tested for the potential healing behavior.

This combination of testing procedures and the materials examined will establish the importance of ionic content to the self-healing behavior. Finally, a proposed mechanism by which healing occurs was determined and is presented in this thesis.

2. Literature Review

2.1 Introduction

Though the copolymer and ionomer materials of this study have existed since the 1960's, only one prior report has addressed the self-healing behavior of these materials and is discussed below. This chapter will provide a brief introduction to ionomer materials and their self-healing behavior. Also, a comparison of the mechanism of healing in these materials versus that of other self-healing systems will be presented.

2.2 Ionomers

Ionomers were defined by *Tant and Wilkes*[2] as a class of ion containing copolymers in which the maximum ion group content is ~15 mol%. Given the lack of distinction between such systems and polyelectrolytes, this definition was further refined by *Eisenberg and Rinaudo*[3] to state that ionomer bulk properties are governed by ionic interactions within discrete regions of the polymer structure.

Ionomers are produced by a unique copolymer neutralization process. They are derived from precursor copolymers containing both ionic (anionic) and nonionic repeat groups. In many cases, the ionic component consists of pendant acid groups attached along the polymer chain. This anionic acid component is then neutralized, resulting in the formation of an ionic pair with a metallic cation. This neutralization process produces the ionomer (or ionic copolymer) with ionic groups as part of the polymer structure. Depending on the number of acid groups neutralized, the amount of ionic content present is said to differ.

With the unique attractions provided by the presence of these ionic groups, ionomers are noted to possess a very unique and interesting microstructural character. The ionic pairs have been shown to group into discrete regions known as multiplets. *Eisenberg*[4] defined a multiplet as "an aggregate consisting of several ion pairs and containing only ionic

material"[5]. Further, according to the EHM model presented by *Eisenberg, et al*[5], these ion pairs anchor their attached polymer chains to the multiplet. This provides a sort of physical crosslink in the polymer structure considerably reducing mobility of the attached polymer chains in the vicinity of the multiplet. This surrounding area is known as the restricted mobility region due to this significantly reduced mobility compared to that of the bulk polymer. A representation of this concept is given in Figure 2-1. For the figure shown, the multiplet is circled in blue at the center of the image. Surrounding the multiplet is the restricted mobility region consisting of the attached polymer chains and extending to the dashed circle as shown. Beyond this dashed circle, the polymer chains return to their typical bulk mobility. From this model, a clearer understanding of the multiplet is obtained.

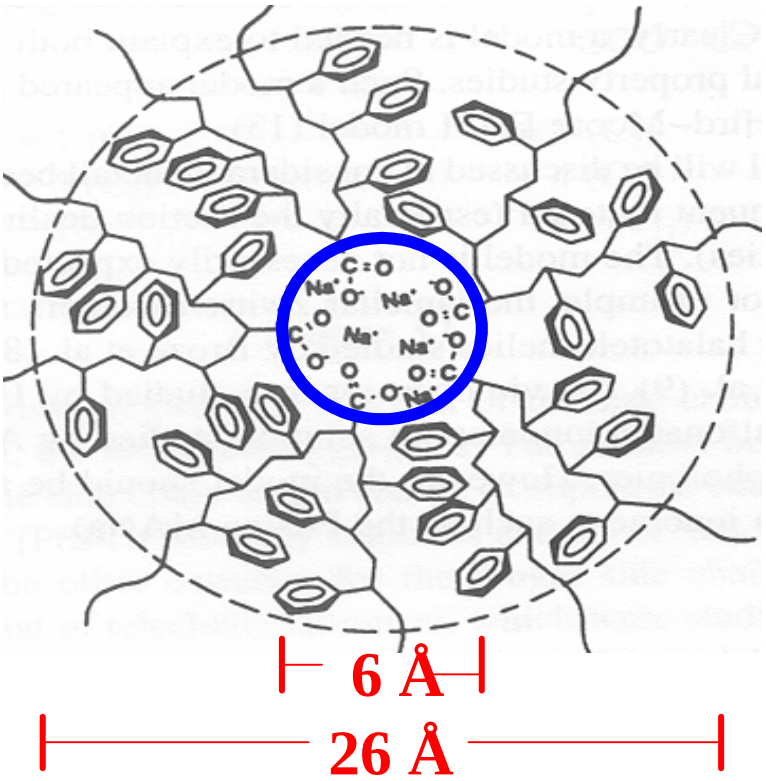

Figure 2-1 Ionic multiplet in poly(styrene-co-sodium methacrylate).[5]

The next step in the ionomer hierarchy described by *Eisenberg, et al*[5] is the ionic cluster. Upon increase in ionic content, more multiplets are created causing them to form closer

together. With this increase in multiplet density, the restricted mobility regions of the neighboring multiplets begin to overlap forming a more continuous restricted mobility region throughout the polymer structure. This new continuous region is defined as the ionic cluster and acts as a second phase within the ionomer, even expressing its own T_g. This concept is described below in Figure 2-2. Here, three regions 'a', 'b', and 'c' are shown, containing differing ionic content. The multiplets are indicated as circles with their surrounding restricted mobility regions given as gray areas. As the level of ionic content is increased from low to high ('a' to 'b' to 'c'), the restricted mobility regions are shown to overlap, producing these clusters.

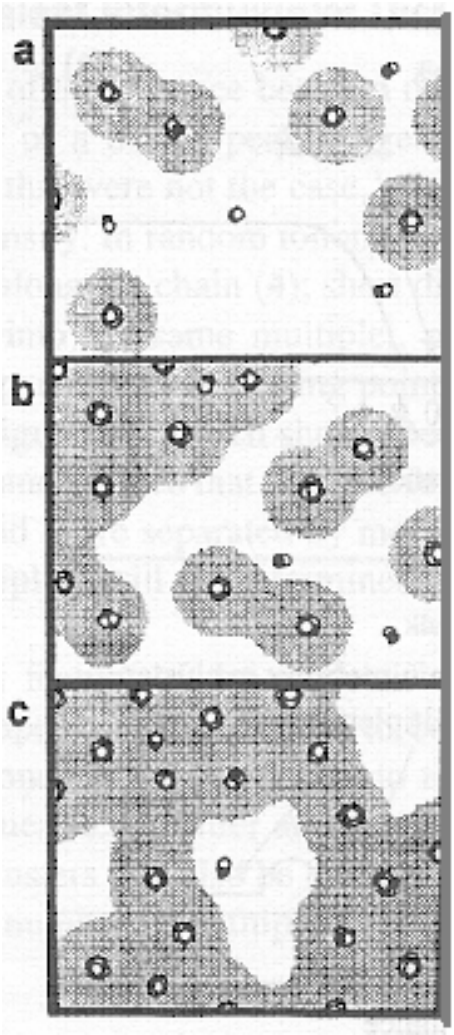

Figure 2-2 Schematic image showing the growth of the restricted mobility region and formation of clusters with increase in ionic content.[5]

Given the significant role of ionic content in determining the unique microstructure, their effects on ionomer behavior are now discussed. It is firmly established in the literature that the amount of ionic content has a drastic effect on mechanical properties[6-9]. In the study of *Bellinger, et al*[6], sodium sulfonated polystyrene ionomers (Na-SPS) showed an increase of ~60% in tensile strength and ~100% in toughness with an increase from 0 to ~7.5 mol% ionic content. For EMAA materials, *Statz*[7] and *Rees*[8] showed a 2-5 fold increase in modulus for ionic acid neutralization levels up to 40%. Further, *Rees* also noted a near 50% increase in tensile strength when neutralization of EMAA was raised from 0 to 80%.

The unique ionic character is also noted to impact thermal characteristics. *Tadano, et al*[10] showed that the ionic clusters exhibit a first-order transition during heating. This transition was located below onset of the T_m of the crystalline regions of the polymer chain and was identified as an order-disorder transition during which the ionic groups disorder upon heating above the T_i. Upon subsequent cooling, it was shown that the ionic groups then reordered over a long time relaxation process with the T_i peak observed to advance to higher temperatures and increase in definition rather slowly. For the EMAA materials studied, the relaxation process was noted to take ~38 days for the peak to revert back to its original size and location. Figure 2-3 below summarizes these thermal events schematically. At left, the ionic groups start in the ordered state as circled in red. Upon increased temperature, they pass through T_i and the ionic regions disorder. With further heating, the polymer crystallites noted in blue melt at T_m. Subsequently, upon cooling through the T_c, polymer crystallites form. When reaching the cooled, room temperature state, the ionic regions remain disordered only to reorder through the long term relaxation process described above while annealing at room temperature

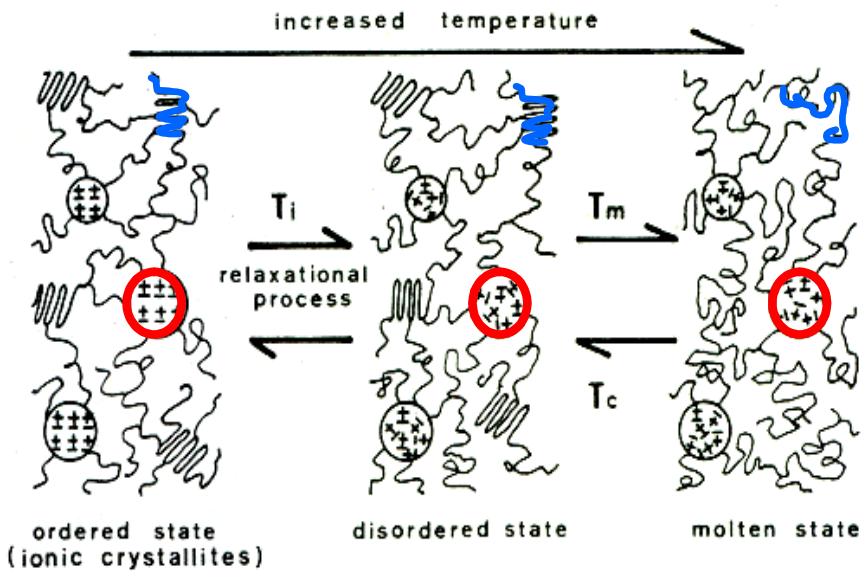

Figure 2-3 Model of thermal effects on ionomer order-disorder and crystallization.[10]

In summary, the ionic character of these ionomer materials plays a significant role in controlling their unique structural nature. It provides them with novel thermal characteristics and produces significantly altered mechanical properties compared to the copolymers from which they are formed. As will be discussed in the following section, it may even facilitate the self-healing behavior in question.

2.3 Prior Self-Healing Studies on Ionomers

As mentioned, the self-healing behavior of the EMAA materials has received little attention in the literature. The M.S. thesis of *Fall*[1] provides the extent of what is published. In addition to some polymer characterization, *Fall* performed bullet puncture tests on React-a-Seal®, Surlyn® 8920, Surlyn® 8940, and Nucrel® 925. The polymers vary in ionic content, with Nucrel® 925 being the only one at 0% neutralization of the acid groups (effectively 0% ionic content). In *Fall*, it was expected that ionic content and its order-disorder transition was the driving force behind the puncture healing process. It was hypothesized that healing would occur if sufficient energy was transferred to the polymer during impact, heating the material above the order-disorder transition and disordering the aggregates. Following puncture and the "removal" of this heat energy,

the ionic aggregates would then reorder causing the ionomer to heal. This idea is shown schematically in Figure 2-4.

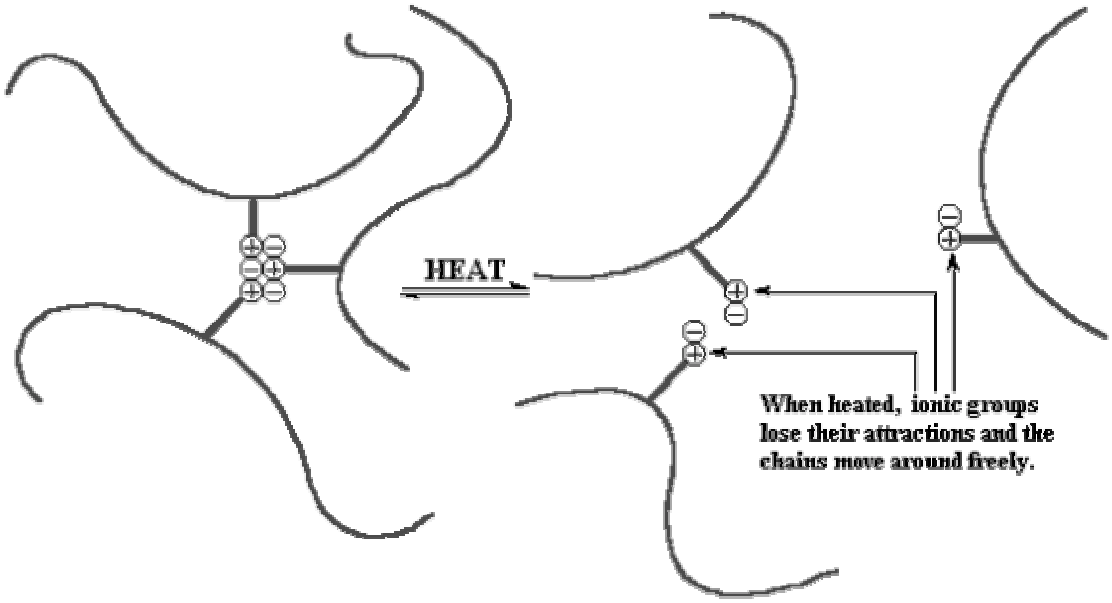

Figure 2-4 *Fall*[1] theory of healing by ordering-disordering of aggregates with heat.[11]

The above hypothesis was initially supported by remote thermal infrared camera imaging of the projectile tests using 9 mm bullets. Figure 2-5 shows an infrared thermogram of a React-a-Seal® film immediately following puncture. This, as well as tests of the other samples, revealed all materials to heat to ~98°C during the impact (~3°C above their melt temperatures). As expected, this temperature increase does produce disordering of the ionic aggregates as well as a localized flow state.

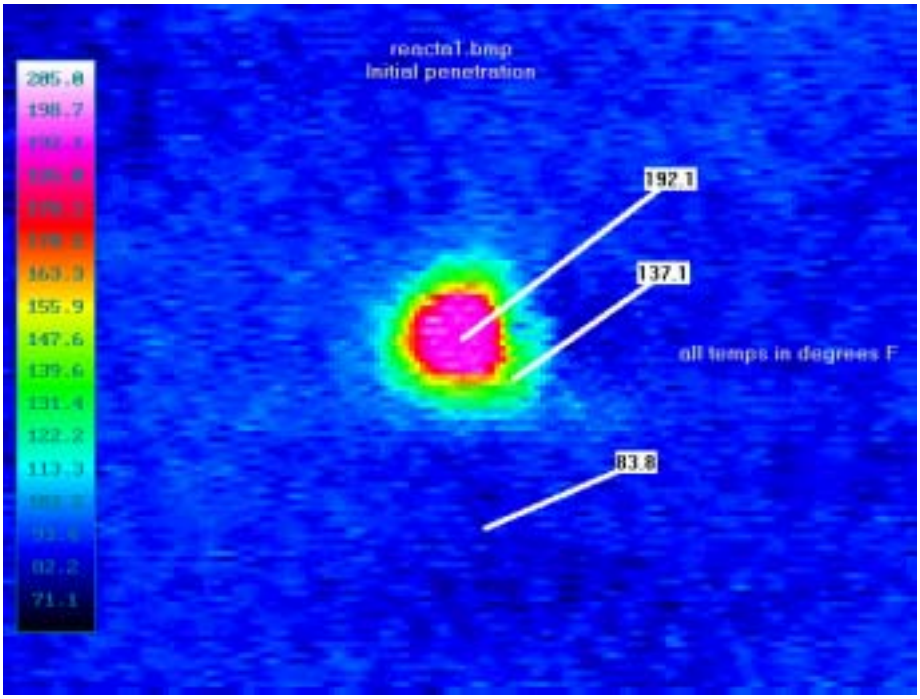

Figure 2-5 Thermal IR camera data from punctured sample.[1]

However, the initial hypothesis of ionic motivation for healing proved inaccurate as bullet testing revealed samples of *all four materials to heal*. Here, samples were found to have healed sufficiently to prevent the passage of water through the puncture site. Given its lack of ionic aggregates, the puncture reversal of Nucrel® 925 determined healing was not solely a result of ionic character as expected. Hence, *Fall* proposed two factors to contribute to the healing response. First, the locally molten polymer indicated by the thermal IR camera suggested that melt flow properties were important to the healing behavior. Secondly, ionic aggregation was said to be necessary. This is surprising given the lack of ionic aggregates in the healed Nucrel® 925, though *Fall* attributed it to the existence of a weak aggregation behavior in the Nucrel® 925 samples. In conclusion, *Fall* proposed that "the increased elastic character of the melt, due to viscosity, primarily drives the healing phenomenon."[1]

2.4 Other Self-Healing Mechanisms and Systems

In order to better understand the healing process examined in this investigation, the reader must first recognize the differences between the mechanism of healing involved in the system in question versus that of a number of other healing systems previously studied. Hence, a description of the different mechanisms of healing, the way the different systems operate and their capabilities, is given.

There are three commonly discussed mechanisms which carry the term "healing" or "self-healing" in their description. These healing mechanisms include autonomous crack-healing via chemical reaction[12], interfacial healing of two discrete surfaces[13-15], and crack and craze-healing,[15] with each operating via the mechanism of either chemical or thermal healing. For each mechanism, there may be several different polymer systems that have been studied which exhibit that particular healing-type response. However none of these effectively describes the EMAA ionomer system studied here or encompasses the capabilities it presents for healing large-scale damage, at great speed, and without manual intervention.

The first self-healing mechanism to be examined involves a chemical reaction causing polymerization to seal a crack that forms in the material. The best known system is that described by *White, et al.*[12] Here, a composite material is fabricated containing monomer-filled microcapsules. As shown in Figure 2-6, upon impingement by a crack (*a*), the microcapsule is burst and the contained "healing agent" flows out filling the crack via capillary flow (*b*). This healing agent then reacts with catalyst embedded in the surrounding matrix and polymerizes thus sealing or "healing" the crack, providing a restoration of mechanical properties (*c*). While this engineered healing composite represents a very exciting advance in the self-repair of materials, it is limited to crack-type damage and would not be expected to heal the large sized projectile damage (several mm in diameter) described in this study of EMAA materials. Of course, the biggest difference between this and the EMAA healing system is the fact that the EMAA system (which is not a composite) is known to heal via a thermomechanical response rather than by chemical reaction.

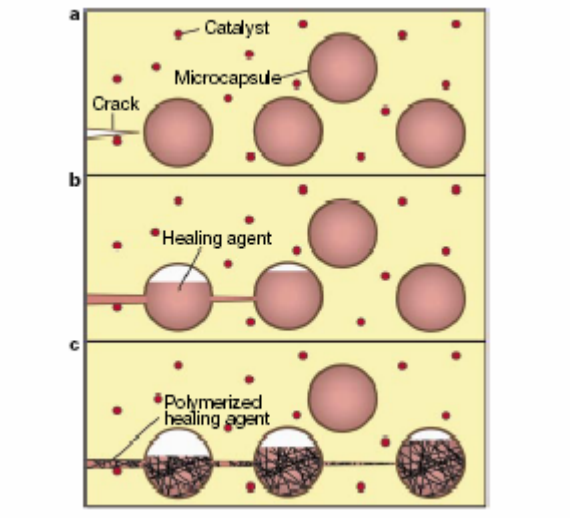

Figure 2-6 Autonomic healing concept.[12]

While the first healing situation pertains to crack healing, the second requires no damage to the material, instead involving interfacial bonding. In this case, as described by *Wool*,[15] "healing" refers to the phenomenon in which two polymer surfaces bond together along their interface when placed in intimate contact above T_g. This phenomenon commonly referred to as "healing" is essentially the interfacial welding of two polymer surfaces. *Wool*[15] states that this healing occurs when polymer chains interdiffuse by motions across the interface. This is accomplished via chain reptation-type motions. This form of healing is commonly studied when polymers are placed in contact above T_g (for amorphous) or above T_m (for semicrystalline polymers) (i.e. welding). However, *Boiko, et al*,[14] have observed some amount of healing in polystyrene and polyethylene terephthalate below T_g. Their results also indicate bond strength to increase with increase in healing temperature. Though this idea of interfacial bonding is quite interesting, there is no damage mechanism involved, pointing out an important difference between this system and that of the EMAA materials studied in this document.

Finally, the third type of healing to examine is that of the thermal repair of cracks and crazes (or other small damage artifacts) as discussed in *Wool*.[15] This process operates via the same theory as the previous mechanism; however a damage component has been

attached. In a number of studies by Wool and co-workers, cracks and crazes in materials were repaired via thermal annealing of a material following damage.[15] Here, a molded polymer sample (for example, polystyrene) was fractured to create a crack. This sample was then heated above its T_g while its surfaces were constrained so as to hinder expansion as shown in Figure 2-7. As the sample heated and expanded, the crack surfaces came into intimate contact and healing could progress following the diffusion process described above, mending the crack. In these studies, healing occurred on the order of many minutes or hours. Yet, in the EMAA system, the observed healing phenomenon occurs in a fraction of a second. Also, there is no external, manual intervention of applied heat to heal the system; rather, the healing response is stored and contained within the system itself. Also, in the ionomers what is being healed is not simply a small crack but a circular hole on the order of many mm in diameter where the interfaces to heal are many mm apart. While reptation motions may lead to sticking/interdiffusion of polymer surfaces, they would certainly not dictate the large scale motions necessary to bring the surfaces back together in the case of puncture healing in the EMAA material.

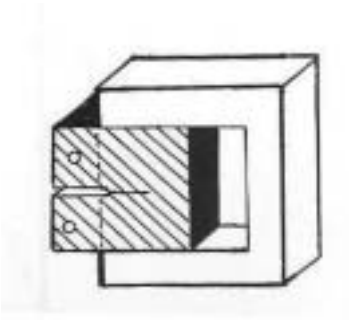

Figure 2-7 Constraining clamp for thermally induced healing of cracks.[15]

Hence, there are very significant differences between the healing mechanisms described above and the self-healing phenomenon taking place in the EMAA materials of this study. In these EMAA materials, healing occurs nearly instantaneously following puncture by a projectile several mm in diameter. Hence, the self-healing phenomenon to be studied involves, specifically, the closing of this large hole and its potential for sealing. It is this very different complex phenomenon that is of interest in this study.

This research asks the question how, why, and on what time scale does this phenomenon occur.

3. Materials, Preparation, and Basic Characterization

3.1 Materials

During the course of this study, four EMAA (ethylene-co-methacrylic acid) random copolymers were examined in order to explore the self-healing phenomenon. These included two EMAA copolymers without ionic neutralization of the acid groups and two EMAA ionomers with partial ionic neutralization of the acid groups. A proprietary EMAA ionomer product, React-a-Seal®, which is based on one of the above materials, was briefly examined. For purposes of comparison, a low density polyethylene was also included.

In a separate part of the investigation, new materials were fabricated. In this research, multi-wall carbon nanotubes were used as a filler material to produce composite samples.

3.1.1 Nucrel®

Nucrel® is the DuPont™ trade name for the thermoplastic EMAA random copolymer. Two varieties of Nucrel® were examined— Nucrel® 925 and Nucrel® 960. Both contain 5.4 mol% methacrylic acid (MA) groups randomly distributed along the polymer chains. The main difference in the two copolymers is that Nucrel® 925 has a greater average molecular weight. A schematic of the copolymer structure is given in Figure 3-1. Nucrel® is commonly used in applications involving footwear, wire and cable coating, metal coating, and glass coating. It is tough and flexible, lightweight in nature, and easy to colorize. Nucrel® was included in this study because it is the non-neutralized base copolymer for the two ionomers described in the following section. It was obtained as a pelletized resin from DuPont™.

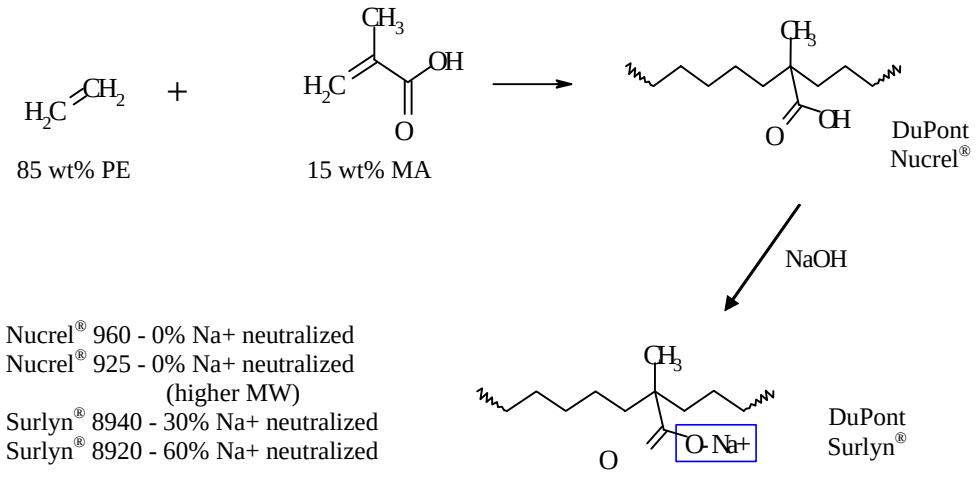

Figure 3-1 Nucrel®/ Surlyn® Chemical Structure.

3.1.2 Surlyn®

Surlyn® is the DuPont™ trade name for a thermoplastic EMAA random ionomer. It is, in essence, the partially neutralized version of Nucrel®. Two varieties of Surlyn® were examined during the course of this study. Both contain 5.4 mol% MA groups; however Surlyn® 8920 has 60% of its MA groups neutralized with sodium cations while Surlyn® 8940 has 30% neutralized by sodium cations. A schematic of their structure is given in Figure 3-1. These two Surlyn® resins are formulated to provide excellent clarity and stiffness with the 8920 having a higher abrasion resistance. Surlyn® resins are commonly used in a number of applications including golf ball covers, hockey helmets and ski boots. Surlyn® resin was obtained from DuPont™ in pelletized form.

3.1.3 React-a-Seal®

React-a-Seal® is a proprietary formula of Reactive Target Systems, Inc. It is based on the Surlyn® 8940 formulation; however, the exact additives to its make-up are unknown. The product is marketed as a self-healing material which seals upon bullet puncture. It is sold as a target material for shooting ranges due to this reusable nature. Because of its unknown formula, it was not examined in-depth during the course of this study. React-a-Seal® was obtained as a 0.25" thickness sheet.

3.1.4 Polyethylene

Low density polyethylene (LDPE) was examined for comparative purposes during the study. LDPE was obtained as a pelletized resin from Scientific Polymer Products, Inc. It has a M_n of 50,000 g/mol.

3.1.5 Carbon Nanotubes

Carbon nanotubes were used as a filler material in composite samples with a Surlyn® 8940 matrix. Specifics to materials selection and fabrication will be discussed in the experimental chapter dealing with these novel composite materials (Chapter 7).

3.2 Sample Preparation

3.2.1 Compression Molding of Polymer Films

Polymer samples were fabricated using a "hot-pressing" process. This method produced polymer films from the pelletized resins of Surlyn® 8940, Surlyn® 8920, Nucrel® 960, Nucrel® 925, and LDPE. The pelletized resin was placed in a stainless steel mold using Dupont™ Kapton® as a release film and allowed to heat in a pre-heated press for 4 minutes at 150°C. A ram force of 40,000 lbs was then applied and held for 30s. Samples were removed from the press and allowed to air cool at room temperature. This process produced very high clarity, smooth polymer films.

These films were tested as prepared or were used in subsequent sample preparation steps for more specific experimentation. Any further preparation procedures for specific testing will be discussed in their respective chapters.

3.2.2 Storage Conditions

All samples were stored in desiccators containing anhydrous calcium sulfate (Drierite®) until testing.

3.3 Standard Characterization Techniques

3.3.1 Introduction

Prior to an examination of the self-healing behavior, some standard testing techniques were employed to characterize the samples produced.

3.3.2 TGA

The TA Instruments Hi-Res TGA 2950 was used to perform thermogravimetric analysis (TGA) on polymer samples. The specific method ramped temperature from room temperature (RT) to 800°C at 10°C/min in a nitrogen gas environment. This instrument allowed moisture content of polymer samples to be determined and provided an understanding of their degradation processes.

3.3.3 DSC

The TA Instruments DSC 2920 was used to examine the thermal characteristics of the polymer samples. This differential scanning calorimeter (DSC) system was equipped with an RCS cooling system and used nitrogen as a purge gas. The specific procedure involved the following:

(1) Equilibrate at 20°C
(2) First Heat to 140°C at 5°C/min
(3) First Cool to 20°C at -10°C/min
(4) Second Heat to 140°C at 5°C/min

This technique allowed examination of thermal transitions for the polymers studied. These included the order-disorder transition (T_i), melt transition (T_m), crystallization transition (T_c), and other thermal characteristics.

3.4 Basic Characterization of Sample Preparation

3.4.1 TGA

Given their ionic character, ionomer materials are hydrophilic in nature, susceptible to moisture content which may have an effect on their structure[16]. While steps were taken to produce consistent samples and minimize storage humidity, TGA was utilized in order to determine any moisture uptake of these materials. Both pelletized resins prior to molding and pressed ionomer films as stored were examined. Three representative samples of Surlyn® 8920 were tested. The first was the pelletized resin from a previously opened factory bag of 8920 which was sealed during storage. The second sample was the desiccator-stored, pelletized 8920 resin. The third was a pressed film stored in a desiccator.

The results of the TGA analysis are shown in Figure 3-2. Testing revealed that pelletized resin as stored in the factory package remained at low moisture content during storage. As noted in the product literature, vacuum oven drying processes should not be necessary unless the bag remains open for approximately one day[17]. The TGA results verified this statement. For samples stored in the desiccator, moisture content was greater—approaching 1.5 wt% gain for pelletized resin and 3 wt% gain for films as measured at 150°C. This difference may arise from a change in the relative surface area of films vs. pellets, or it may be a result of the samples being stored in different desiccators. The pelletized resin was stored in a "wet seal" desiccator while the film was stored in a "dry seal" type desiccator. It is possible that the different sealing mechanisms for the desiccators led to differences in storage humidity. With regard to final quality, in all three cases, it was noted that most of the moisture was lost from the samples when temperature reached 150°C. This suggests that the 4 minute "hold-step" of the

compression molding process was sufficient in eliminating most of the moisture from the samples. The high consistency of samples produced, lack of problems with moisture bubbles, and TGA data prove moisture was not a problem in the samples produced.

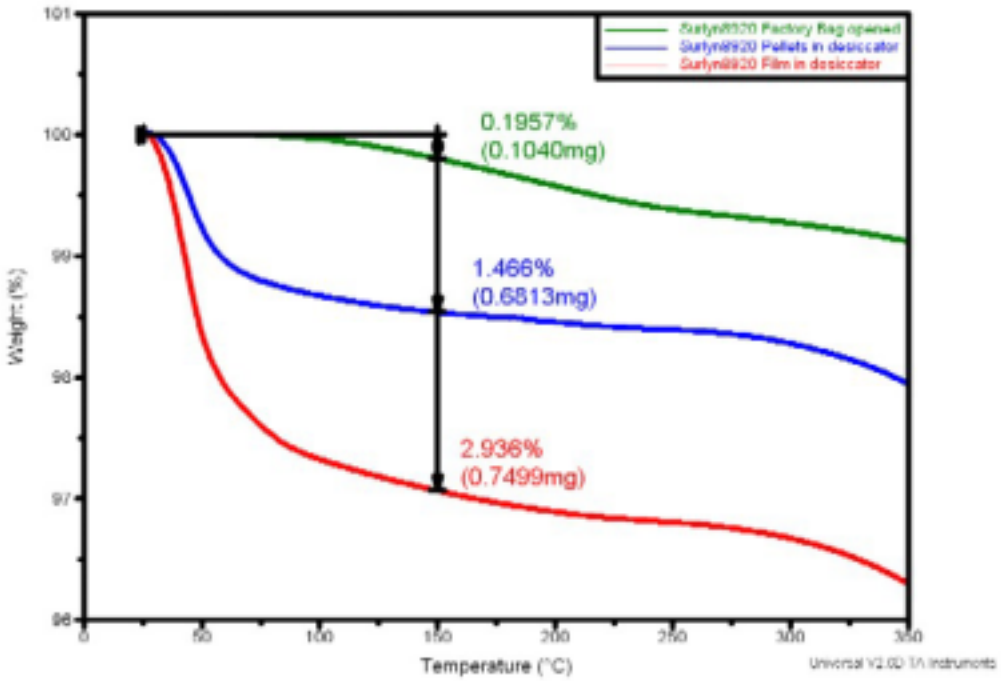

Figure 3-2 Moisture content of Surlyn® 8920 samples given by TGA analysis.

3.4.2 DSC

Information obtained during the DSC first heat of polymer samples allowed verification of T_m, T_i, and the ordering of ionic clusters with aging time. Testing was performed on Surlyn® 8940 films after three different aging periods—2 hours, 2 days, and 1 year$^+$ after their thermal histories were erased by heating them above the T_m. During subsequent testing, the T_i peak was observed to grow and shift to higher temperatures with longer aging times as shown in Figure 3-3. The growth in this peak indicates ordering of ionic clusters on aging. This trend is consistent with previous studies investigating the order-disorder transition[10, 18, 19]. The peak value of the order-disorder transition was observed to reach a maximum at 50.7°C. This is near the T_i value of 51.9°C determined by *Fall*

using DSC[1]. The melt transition, T_m, was observed to peak at ~ 94°C which is also near that measured by *Fall* (~95°C).

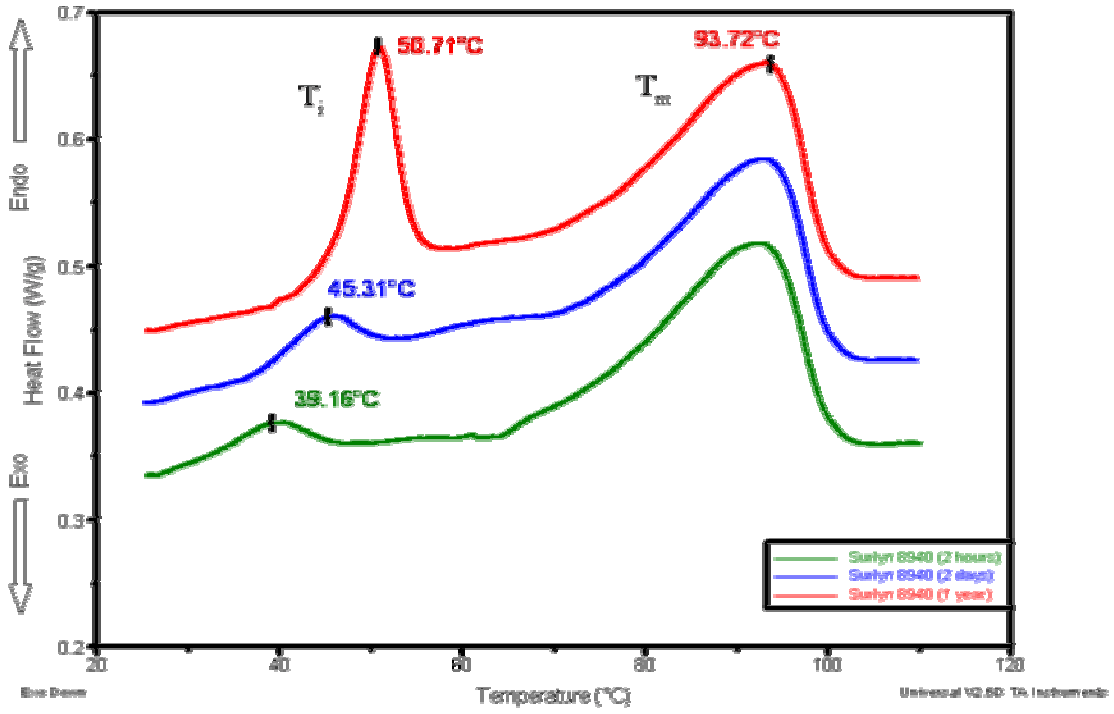

Figure 3-3 DSC of aged Surlyn® 8940 films. Order-disorder peak is shown to shift to higher temperatures and grow for aging times of 2 hours, 2 days, and 1 year. T_m is also noted at ~94°C.

3.5 Other Experimental procedures

Beyond these standard characterization techniques, several other experimental procedures were employed in understanding the self-healing behavior of ionomer materials. These testing procedures and their details will be discussed in the following chapters.

4. General Self-Healing Response

4.1 Introduction

In this chapter, several general observations on the self-healing process are discussed. While the self-healing response was observed to occur in films of the ionomers during some modes of damage, under other conditions it did not take place. The results of this chapter provide a better understanding of the healing phenomenon based on an analysis of the facts.

As determined by *Fall*, self-healing characteristically occurs almost immediately following projectile (bullet) puncture[1]. This is confirmed below and some revealing new puncture experiments are discussed. Furthermore, several other damage methods were also examined and general observations on their results in healing are given. These include damage techniques such as sawing, cutting and various puncture methods.

4.2 Damage Modes

4.2.1 Projectile Impact

Ideally, the self-healing process would result in punctured films showing no evidence of having ever been ruptured. The specific tests conducted by *Fall* did not show this to be true[1]. Instead, a residual "scar" was observed at the puncture site. Even with this scarring, it is said that healing has occurred because no continuous, surface-to-surface hole remains. Thus, the puncture is tightly closed and impenetrable to liquid.

In the current research, projectile testing was conducted using a Crosman® Model 664GT, 0.177 caliber (4.5 mm) pellet air rifle pumped to the maximum pressure (10 pumps) which yielded a projectile speed of about 182 m/s. Films with a thickness between ~0.8 and ~1.6 mm were punctured. The healing response to three different projectile geometries was examined. In another experiment, multiple penetrations at the same

location were studied to determine the potential for "re-healing". One test examined the puncture of two films in contact to evaluate whether they might heal together. Lastly, LDPE was punctured and compared with the self-healing response of Surlyn®.

4.2.1.1 Projectile Shape

Three different projectile shapes were assessed for eliciting self-healing in Surlyn® 8940 film. These Crosman® projectiles were a spherical BB, a flat-headed "Super Match" pellet, and a bullet-shaped "Pointed" pellet. Upon impact, each produced a unique response.

The first, a spherical BB, failed to puncture the film, instead forming a pocket. Here, the film stretched to conform around the BB's shape leaving a circular opening to the impact side of the film that was smaller in diameter than the BB, and trapped the BB inside this cavity. This smaller diameter opening may reflect an attempt to heal around the BB.

The second projectile, the flat-headed pellet, punctured the film. However it was trapped as the film healed very quickly catching the pellet by the neck between its flat head and flared tail. This result indicates that the healing event has a very fast response time.

The third projectile was the pointed pellet. Though this projectile also had a neck as did the flat-headed one, it fully penetrated and exited the film, leaving the sample healed. A scar was noted at the site. A representative image of the healed puncture and scar is shown in Figure 4-1. This scar was noted to be smaller in diameter than the projectile which had impacted it. This indicated a recoverable drawing without fracture of the localized perimeter of the film during puncture. During puncture, the different impact geometry of the pointed projectile had wedged the film open and was allowed to escape without being caught as was the flat-headed projectile described above. The exact difference in the impact dynamics between the two shapes is not fully known. As a result of this test, the pointed pellet was used in all further testing.

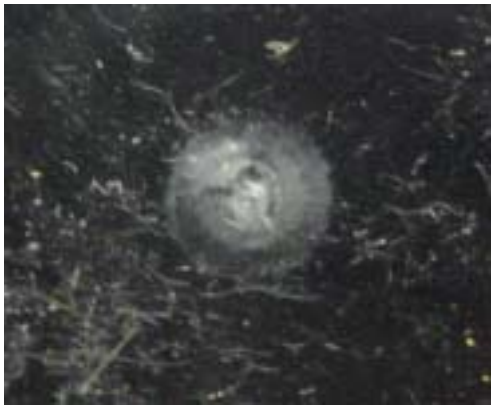

Figure 4-1 Residual scarring at healed puncture location in an ionomer film following high speed penetration by a pellet.

4.2.1.2 Multiple Punctures

For this test, a ~0.8 mm thickness film of Surlyn® 8940 was punctured. The film was shot a second time at the same location and was again observed to heal. The same was done with a ~5 mm offset for the second shot and that site also healed. This simple test demonstrated the ability of the films to re-heal upon a second puncture, though details as to their abilities upon further punctures are unknown. Given the scarring left on the punctured samples, the permanent damage suggests there would be a definite limit to the number of healing events the material can sustain. However it is also believed that different testing conditions (speed, film thickness, temperature) could produce little or no scarring, resulting in the expectation of unlimited "re-healing" potential.

4.2.1.3 Puncture of Multiple Layers

In this case, two ~0.8 mm thickness films of Surlyn® 8940 were shot while the films were held in contact. These films were observed to heal and were adhering to one another with a pivot point about the healed hole. This point allowed rotation between the films yet provided an elastic resistance to their twisting. Whether this was a mechanical interlocking of the punctures or a combining of material from both films is not known. Thermal IR camera data from *Fall* suggests that samples heat to above their melt state

upon puncture/healing[1]. Hence, it is expected that the two films were most likely fused together at the healed site.

4.2.1.4 LDPE

As polyethylene comprised 85 wt% of each of the EMAA copolymer materials in this study, 100% LDPE films were shot for comparison. The LDPE samples did not express the healing response. Instead, as seen in Figure 4-2, the film was observed to draw with the initial impact and then fracture by removing a "cap" of film attached to the pellet tip as shown in the side view image. This fracture mechanism does not occur in the self-healing materials. Instead, as observed for the different projectile shapes tested above, the self-healing films manage to puncture allowing the projectile to pass while conserving material to fill the hole. By some means the film then recovers to close the void volume. This lack of self-healing in LDPE indicates the importance of the ionic functionality, or at least the very polar acid groups contained in the EMAA materials, in producing the self-healing behavior.

Figure 4-2 LDPE punctures—healing did not occur. Side view (left) and back view (right). The cap of film ejected with the projectile can be seen in the side view image.

4.2.2 Sawing

In this videotaped experiment previously unreported by *Fall*, a ¼" thick sheet of React-a-Seal® roughly 10 cm x 25 cm was mounted in a vise and sawed through with a hacksaw. During sawing the ionomer was observed to heal behind the blade—the two halves immediately reforming behind the saw blade. Upon completion of the cut, the halves

were fused together with a spring-like, elastic hinge. Four images from a video of the process are shown in Figure 4-3. They progress in time clockwise starting with the upper-left image. During sawing, a great deal of heat was generated in the React-a-Seal®. The material responded by "gumming up" in a molten state, filling the void behind the saw. Not only did it bond the two pieces together, but it made sawing very difficult. This correlation of heat with healing behavior is consistent with results from the thermal IR camera data of *Fall*[1] and emphasizes the importance of heat energy in eliciting the healing response.

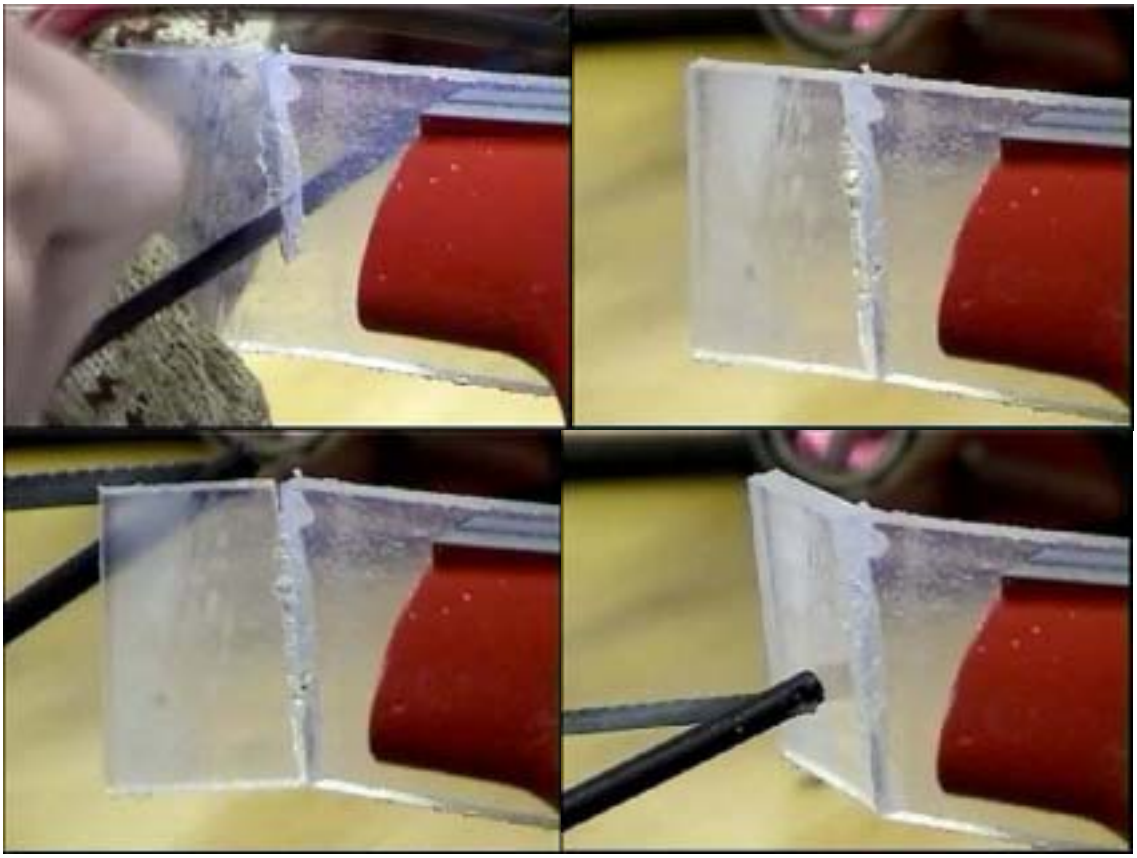

Figure 4-3 Self-healing of sawed React-a-Seal®. Images progress clockwise from the upper-left. Upon completion of the full cut, the two pieces are healed together and provide an elastic bond between the two pieces.

4.2.3 Cutting

While sawing produced the healing behavior, cutting of samples elicited no such similar response. In the course of the study, numerous samples of varying thickness (below ~ 2 mm) were cut by scissors or razor; however no self-healing behavior was ever observed. During sawing experiments, heat was generated through friction in the sawing process. This however was absent in cutting by scissors or razor. This supports the idea that the damage mechanism must be a high energy process which generates heat in the material.

4.2.4 Nail Puncture

A film of Surlyn® 8940 was punctured by driving a nail through the sample. Upon removal of the nail several seconds later, no healing was observed. Given the observed high speed of healing during the projectile tests, it is expected that the delay in removing the nail hindered the healing response by producing permanent deformation of the film through polymer relaxations. Hence, not only does healing demand an energetic puncture process but also that the puncture occurs as an unsustained, momentary event.

4.2.5 Sewing Needle Puncture

Very thin films (0.5 mm) of Surlyn® 8940 were punctured by sewing needle using a sewing machine. This puncture produced a very small scar. However, given the small nature of the puncture, it was not determined whether healing occurred.

Table 4-1 Summary of healing behavior for various damage modes.

Damage Mode	Healed
Projectile Impact *(pointed pellet)*	Yes
Sawing	Yes
Cutting	No
Nail Puncture	No
Sewing Needle Puncture	Inconclusive

4.3 Conclusions

Given the general results summarized in

Table 4-1, it was concluded that high-energy events, which both store energy in the film recoverably and contain an associated non-recoverable high friction component leading to heating of the materials, are more favorable to healing. In the cases of sawing and projectile impact, energy was transferred to the material generating heat. Then by some means, this material recovered to fill the damage site—whether this is due to ionic interactions or other behavior is yet unknown and will be examined further in the coming chapters. In the case of punctures, a shorter, momentary impact is proven necessary. The test on the flat-headed projectile served to show how fast the healing event occurs. However, the nail puncture experiment did not possess this necessary brevity—it did not occur as a quick, discrete event. This allowed the puncture site to permanently deform before the nail was removed. In summary, high energy, heat producing damage modes with short durations are determined favorable to eliciting the self-healing response.

5. Peel Testing of Surlyn® 8940

5.1 Introduction

As noted by *Fall*, impacted ionomer films were observed by remote thermal IR camera to heat to ~3°C above their melt temperature of 95°C during the puncture/healing event[1]. This raises the question of whether or not simply increased temperature may be sufficient to elicit the self-healing response of these materials. To test this idea, two ionomer films were held in contact for 30 minutes at various sub-melting temperatures. A peel test between the two films was then used to examine the level of bonding which occurred between them. The temperature at which bonding (or self-adhesion) may begin to occur could then be determined.

The testing of healing in this manner is very different from an examination of projectile tests that involve damage. Whereas punctured films may reflect a type of "shape memory" in leading to healing, this situation involves two separate films having no initial connection to the neighboring surface—the potential for a "memory" response is excluded. Furthermore, there is no damage to the material involved in the experiments; rather pressure is applied normal to the films in making the "sandwich". In this peel test, it was desired to quantify the healing behavior by bonding films together in response to only an increase in temperature and pressure. If a bonding response is observed, it would provide evidence of an attractive component promoting healing of punctures in these ionomers. From this, it might be extrapolated that this attraction may be critical to the healing of punctured films. Favorable adhesion results could also indicate a sealing behavior occurring during the healing process of projectile punctured films.

There is evidence that these materials do begin to bond together below the T_m. According to the Surlyn® Resin Molding Guide provided by Dupont™, during drying processes, "Oven temperatures should not exceed 65°C or the molding pellets will block and fuse into a solid lump."[17]. During the course of this research no pellets have fused

together during storage at room temperature. However, elevated temperature may provide the mobility necessary for this process to occur at a faster rate. This would be feasible as viscoelastic polymers typically express this type of time-temperature relationship.

Thermodynamics and kinetics are involved in the self-adhesion of polymers. Thus, theoretically, the questions are whether the polymer chains have enough free energy benefit to interdiffuse across their surface boundaries and sufficient mobility to do so at sub-melt temperatures. Given that these are ionic copolymers, the ionic group attractions and their tendency toward forming clusters may be expected to drive this interdiffusion. Ideally, it would be interesting to determine the extent to which this occurs and whether there are clusters formed containing polymer chains from both discrete films. While this test will not examine those behaviors specifically, the measured bond strength will provide an understanding of the relative level of interdiffusion.

In order to assess the above ideas, a 90° peel test was used to measure the adhesion or self-adhesion between Surlyn® 8940 films bonded at constant pressure over a range of sub-T_m temperatures. The debond force was recorded and results are presented below.

5.2 Sample Preparation

The peel test specimens consisted of a flexible peel arm welded to a rigid polymer/aluminum substrate. They were bonded together under varying temperature conditions prior to testing. A photograph of the bonded sample is provided in Figure 5-1.

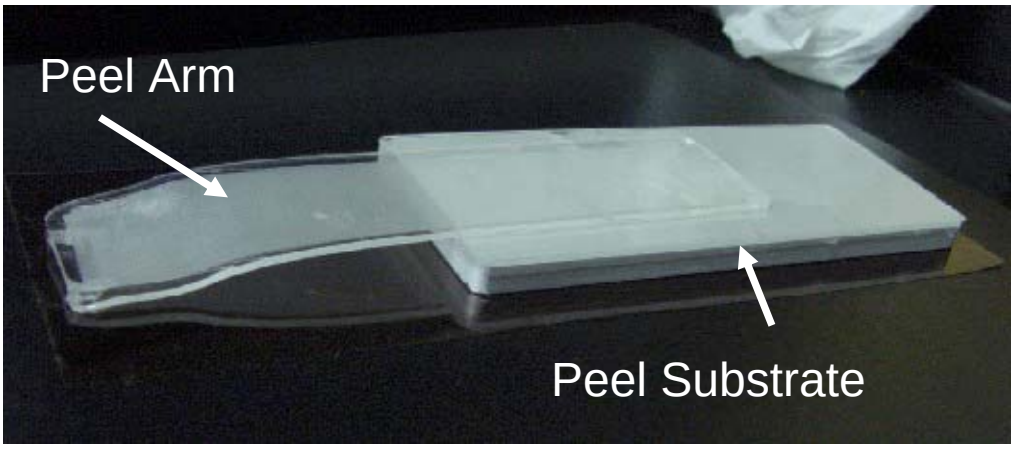

Figure 5-1 Peel test specimen.

5.2.1 Peel Arm

The peel arm included two ~0.8 mm thick laminates of Surlyn® 8940. These laminates were prepared as described in Section 3.2.1. A glass fiber scrim cloth layer was placed between the laminates in order to reduce yielding of the peel arm during testing. Following the same compression molding process, these three layers were fused into one continuous piece producing the peel arm shown in Figure 5-1.

5.2.2 Peel Substrate

The substrate was composed of a ~1.6 mm thickness Surlyn® 8940 film bonded to an aluminum plate. The film, produced using the molding process described in Section 3.2.1, was bonded to the top of the plate using the same compression molding technique. Prior to bonding, the aluminum plate was cleaned and surface treated in order to produce a new, strong oxide layer ensuring rigid bonding of the attached polymer. This surface treatment consisted of the two consecutive procedures outlined below[20-22]

Acid-Base Wash

1. Panels were submerged in acetone at room temperature multiple (3 to 4) times and abraded using Scotch-Brite™ pads in order to remove surface oils and lubricants. Between each cleaning, samples were allowed to dry in air.
2. A new oxide surface was then prepared by submerging the panels in a 5% (w/w) NaOH solution at 50°C for 3 min.
3. Panels were removed from the solution and submerged in 50% (v/v) deionized water/concentrated HNO_3 solution at room temperature for 2 min.
4. Following removal from the acid solution, panels were submerged in deionized water for 2-3 minutes after which they were rinsed in flowing deionized water.

P2 Etch

1. Following the above procedure, the panels were submerged in a P2 solution (122.5 g of $Fe_2(SO_4)_3 \cdot 4H_2O$ + 0.185 L concentrated sulfuric acid diluted to 1 L with deionized water) at 65°C for 8 min. They were then rinsed in running deionized water for 2-3 minutes.
2. Panels were dried at 110°C for 30 min then stored in a desiccator prior to bonding.

5.3 Procedure

5.3.1 Bonding

The peel arm and substrate were bonded together with the ionomer surfaces in contact. This was accomplished by holding the two components together using a minimal amount of contact force (~2.63 psi). They were placed in an oven and allowed to weld for 30 minutes at temperatures of 70, 75, 80, 85 or 90°C. This produced samples as shown above in Figure 5-1. These were stored in a desiccator until testing. Two sets of samples were examined—one set tested an hour after bonding, while the other after 4 days. The bond width was approximately 17-19 mm.

5.3.2 Peel Test

Samples were mounted in a 90° peel test fixture and pulled at a constant rate of 5 cm/min at room temperature using an Instron® 5500R Model 1123. This fixture allowed the peel specimens to slide along a track during testing in order to maintain the 90° peel geometry throughout the experiment. A schematic of the test setup with photograph is given in Figure 5-2.

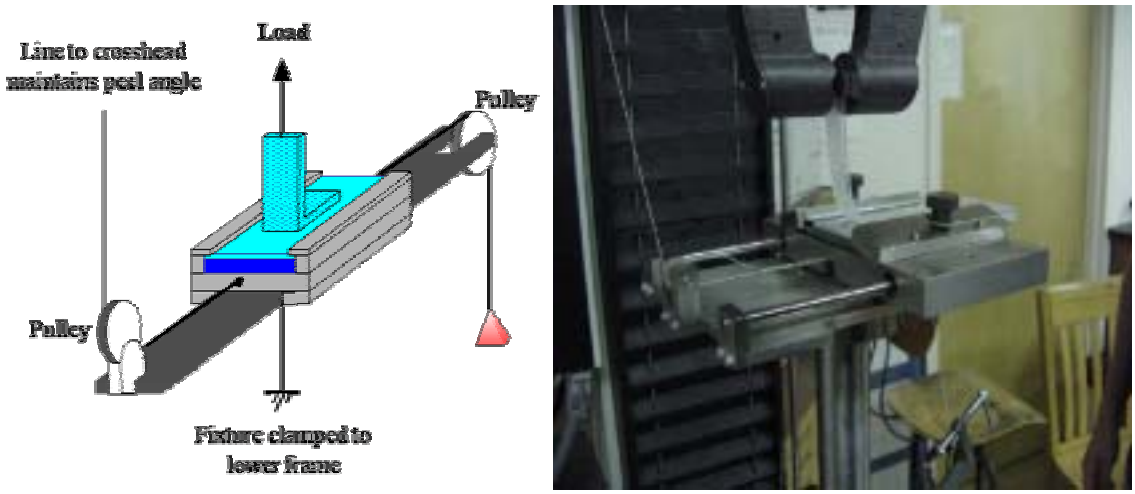

Figure 5-2 Peel test fixture with schematic.

5.4 Results and Discussion

The average peel force for each bonding temperature was calculated and is plotted below in Figure 5-3. For the 70 and 75°C samples, peel angle stayed well below 90° indicating a low bond strength. Here, bonding was too weak to allow bending of the peel arm. Samples bonded at 80°C and above produced debonding close to the 90° bond angle. This indicated a more substantial bond strength as given in Figure 5-3. As expected, the bond strength increased as the bonding temperature approached the melting point. It is noted that bond strength does not increase significantly until ~ 85-90°C for the 1 hour test and at 90°C for the 4 day test. This indicates healing is more complete at these

temperatures. The trend of increased bond strength with increasing temperature is expected as the chains have more mobility at increased sample temperatures.

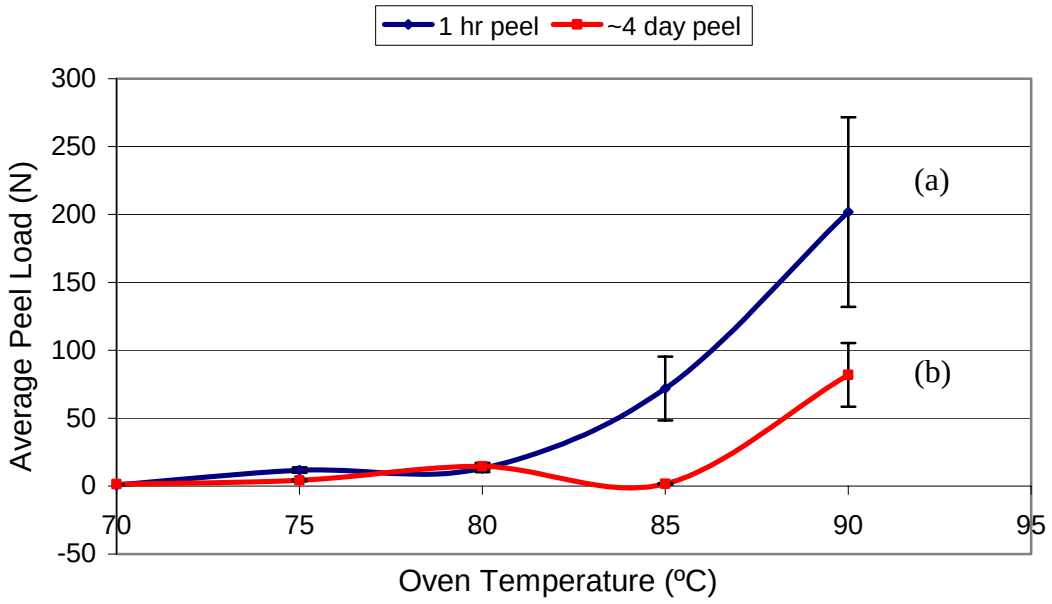

Figure 5-3 Average peel load as a function of bonding temperature for (a) samples peeled after 1 hour, (b) samples peeled after 4 days.

At bonding temperatures below 80°C, bond strength was observed to be relatively weak. As noted in the Surlyn® Resin Molding Guide, the pellets fuse when heated above 65°C; however, this assumes allowing the process several hours to occur[17]. The low bond strength in the cooler samples may reveal a time dependency involved in the bonding process such that longer bond times increase bond strength. This would be consistent with the time-temperature relationship of viscoelastic polymers. It is expected that more significant bonding of the films would occur if bonding time increased, though it is unknown if the samples bonded at lower temperatures would indeed increase their bond strength above that of a 30 minute bond time.

With regard to aged samples, the bond strength decreased with longer aging times. This loss of bond strength may well be the result of humidity that may attack the bond itself, of residual stress, or of a longer term relaxation process such as ordering of the ionic

clusters. As noted in several sources, ionic clusters order during the first few days after an increase above the T_i[10, 18, 19]. This is also noted in Figure 3-3. As testing exceeded T_i (~51°C), this relaxation is the likely cause.

5.5 Conclusions

The peel test indicated that interfacial welding was weak until bonding temperatures increased to within 10°C of the melt temperature. By successful fusing of ionomer films at temperatures near those reached in projectile impact and over reasonably short times, the results indicate the existence of a potential sealing component in the healing mechanism of punctured films. This would act to fuse the puncture perimeter back together sealing the hole. It may also be expected that self-healing will occur more completely (that is, without the scarring seen in the healed projectile puncture samples) if punctured at already elevated temperatures. It is expected that the greater temperatures would provide the films with an increased self-adhesion as indicated in these results and greater mobility to patch the hole. However, there would be a greater chance for material loss during fracture due to lower elongational melt fracture strength. Projectile tests will examine the effect of temperature on the healing event to test this hypothesis.

6. Projectile Testing

6.1 Introduction

Controlled projectile testing on ionomer films was conducted in order to better understand the mechanism of self-healing expressed by EMAA materials following puncture. By examining samples with varying amounts of neutralization, the importance of ionic content to the healing behavior could be determined. Also, by shooting samples at elevated temperatures, further data on the self-healing process and its limitations was obtained in order to aid in modeling of the events.

Unexpectedly, *Fall* showed that even the non-neutralized Nucrel® 925 would heal following puncture[1]. This suggested that ionic content is not necessary to the self-healing process. However, the results need confirmation as the study lacked adequate verification of the "quality" of healing following puncture—samples might have "appeared" healed visually yet may not have fully closed, containing a hole not detected by the assessment process. The deficiencies of the verification procedure used are discussed below in Section 6.3.2.

In the present study, a novel technique for the assessment of puncture healing is utilized. This method not only effectively determines the quality of healing that has occurred in polymer films, but also facilitates a quantitative measurement of their healing quality by determining the "strength" of the healed site. This provides a comparison of the healing behavior between materials of varying ionic content, allowing the importance of neutralization to self-healing to be determined. Also, the inclusion of both Nucrel® 925 and 960 to this study (vs. only Nucrel® 925 in *Fall*[1]) provides an additional non-neutralized EMAA copolymer for comparison.

It has been shown extensively in the literature that the amount of ionic content has a profound impact on the mechanical properties of ionomers[6-9]. This is certainly expected to hold true for the unique property of self-healing. It is believed that ionic content

promotes the healing behavior. Even if healing does occur for all materials of the study regardless of ionic content, the quality of their healing is likely to differ greatly given the increased tendency of the ionic groups contained in Surlyn® materials to segregate as physical crosslinks which the Nucrel® lacks. Their increased self-attraction is believed to produce a strong driving force toward recovery during healing that may be weaker or absent in the non-ionic materials.

As shown, the local material at the puncture site heats to the molten state upon impact[1]. It is theorized that this locally molten polymer maintains an elastic memory of the prior shape due to these ionic regions and their unique attractions—this drives the healing process, closing the hole. Given this hypothesis as well as the increased self-attraction and interdiffusion expressed at elevated temperatures (Chapter 5 Peel Test), it was speculated that the shooting of already heated films will cause samples to heal more completely. They were expected to have less scarring at the puncture site and greater strength of the healed hole compared to room temperature tests.

Puncture testing was performed on films of varying ionic content at room and elevated temperatures. They were then assessed for complete healing and the strength of the healed puncture site was measured. Also, DSC analysis was performed on the puncture site as well as remote areas of the films in order to understand the thermal changes induced by the puncture process.

6.2 Puncture-Testing Instrumentation

A projectile test station was developed in order to conduct projectile testing experiments in a laboratory testing environment. This station also facilitated the shooting of samples at controlled, elevated temperatures. A schematic image of this testing station is given in Figure 6-1. EMAA films were mounted in the sample holder shown and placed in the oven in front of a backstop with the door closed. In order to maintain constant temperature, shooting took place through a window in the oven door. Films were shot using a Crosman® Model 664GT, 0.177 caliber (4.5 mm) pellet air rifle pumped to the

maximum pressure (10 pumps). The Crosman® Copperhead® 0.177 caliber (mass ~0.51g) pointed pellet was used for all testing. This yielded a projectile speed of ~182 m/s with a momentum of ~0.093 kg m/s.

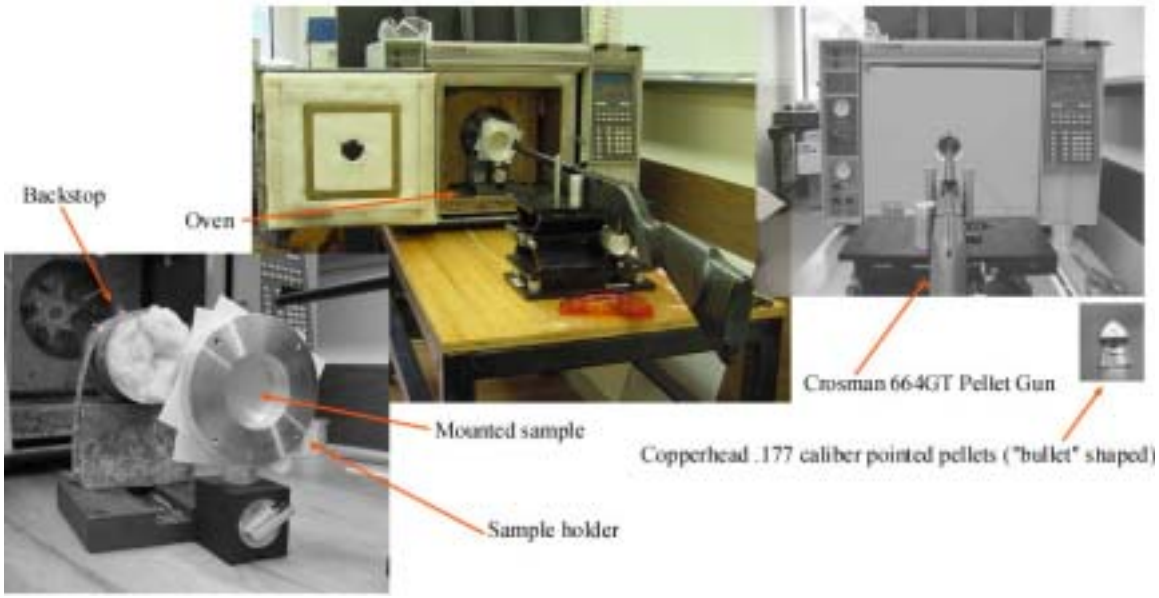

Figure 6-1 Projectile testing station.

6.3 Procedure

6.3.1 Projectile Puncture

In order to compare the effects of ionic content on the self-healing behavior, thin film samples of all four DuPont™ EMAA materials were studied (thickness ~0.85-1.04 mm). Recall, these materials vary in ionic neutralization from 0% for the Nucrel® materials, to 30% for Surlyn® 8940, up to 60% for Surlyn® 8920. Sample films were loaded into the testing fixture and placed in the oven at the testing temperature. They were allowed to equilibrate to test temperatures of 60, 70, 80 and 90°C for 5 minutes prior to shooting. Room temperature tests were also conducted but without this delay. Once shot, they were removed from the oven and examined.

6.3.2 Healing Assessment

Following puncture, samples were assessed for healing. This was accomplished by two different methods—visual and via penetration experiments. The visual method was simple examination by the naked eye. Samples which had clearly not fully healed were noted. The remaining samples underwent further inspection using experimental means.

Initially, the remaining samples were evaluated using a simple liquid penetration test (LPT) similar to the analysis performed (though not explicitly defined) by *Fall* using water [1]. During the LPT a drop of food coloring was placed on the impact side of the puncture site. Filter paper was placed on the reverse surface. If after 30 minutes the filter paper was stain-free, the sample was concluded to be healed. However, following some use of the LPT, potential deficiencies in its reliability were noted. During liquid testing, a high contact angle was observed in the droplet of food coloring on the sample film. This suggested surface tension could prevent the liquid from flowing through punctures that were not fully healed, resulting in a false positive indication for the healing behavior. In fact, a test on a sample known to be punctured but not completely healed proved this to be the case. This result rendered the LPT test no more accurate than the visual technique described above. It also raised the question when healing had indeed occurred in the samples tested by *Fall*[1]. Hence, a more reliable method had to be devised.

A more accurate and useful test was developed which minimized the potential for error shown by the LPT. This novel technique was the pressurized burst test (PBT). It not only assessed whether samples were fully healed (air tight), but also provided a quantitative measurement of their healing quality by measuring the strength of the healed puncture. During this test, punctured sample films that had passed visual evaluation, were mounted in the testing device and loaded on the impacting side via air pressure using nitrogen gas. The exit side was immersed in deionized water. If the film was able to hold an increase in air pressure without leakage, then the sample was determined to be healed. A non-healed sample was indicated by immediate passage of bubbles through the puncture site upon pressurization. Next, air pressure was increased at ~100 psi/min until

the puncture site burst as shown in Figure 6-2. The pressure at failure was recorded. This provided a measure of the "strength" of the healed puncture site, allowing a quantitative comparison of healing quality between the different materials.

Figure 6-2 The sample film is mounted in the window of the test fixture. Upon increased air pressure, failure of the puncture site is indicated by air bubbles escaping into the water bath.

6.3.3 DSC

Following puncture-testing, DSC analysis was utilized to examine the effects of the puncture/healing event on the thermal characteristics of the sample materials. Given the expectation that ionic content was important in self-healing, the specific effect on the order-disorder transition of the ionic clusters was of interest. The same DSC setup as described in Section 3.3.3 was used. The test procedure consisted of the following:

(1) Equilibrate at 20°C
(2) First Heat to 120°C at 5°C/min
(3) First Cool to 20°C at -10°C/min
(4) Second Heat to 120°C at 5°C/min

DSC analysis was applied to samples removed from two different locations of the shot films. The first tested material at the puncture site. For healed samples, this was the healed material itself. For non-healed samples, it typically consisted of the plug of material ejected from the film or the material around the remaining hole. The second material examined was taken from an undamaged location well away from the impact site. This sample served as a baseline for comparison as it had an identical thermal history to the first location lacking the history produced by the shot itself. By comparing the first DSC heating curves from the two materials, the effect of the puncture/healing process on the thermal character of the polymer was determined.

6.4 Results & Discussion

6.4.1 Room Temperature Puncture

Upon shooting at room temperature, *all EMAA materials were observed to heal*. This means neutralized and nonneutralized specimens both showed recovery at 25°C. Images of representative samples are provided below in Figure 6-3. As shown, all healed with the characteristic scarring of the healed site. No significant difference in healing ability can be determined from their appearance. Healing was initially confirmed via the LPT, and then verified using the pressurized burst test. Hence, it was proved that not only did samples containing ionic groups have the ability to heal sufficiently to stop pressurized gas penetration but their non-ionic base copolymers expressed the same behavior.

However, the pressurized burst test revealed inconsistencies as three of six Surlyn® 8920 samples and two of six Nucrel® 960 samples failed the PBT. Of these, two of the 8920 and one of the 960 samples failed prior to pressure being registered by the test gauge, though they may have actually held pressure lower than the minimum recordable amount of 40 psi. Even so, as will be seen in a full discussion of the PBT results, this pressure level is much lower than typical failure levels recorded for the rest of the samples. Hence, the assessment that these low burst pressure samples have not healed is

maintained. As for the other failed samples of these materials, they were unable to hold any pressure as evidenced by "bubbling" prior to any increased loading by the test equipment.

The results of the room temperature tests reveal that ionic neutralization is not necessary for healing. However, its contribution to the healing process cannot yet be ruled out. Whether or not it improves the quality of healing will be discussed further by considering the quantitative pressurized burst data in Section 6.4.3 below.

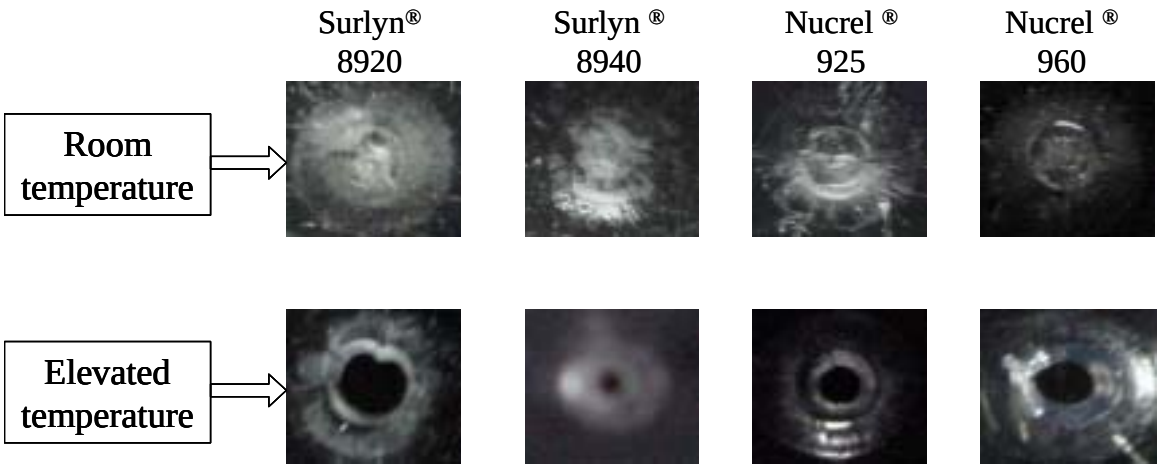

Figure 6-3 Images of the puncture site for the four EMAA materials after tests at RT and typical results at elevated temperatures.

6.4.2 Elevated Temperature Puncture

Elevated temperature testing of films also yielded some surprising results. In light of data obtained from the peel test, it was expected that samples would be more inclined to heal at higher temperatures. The ability of the polymer to fuse together would produce stronger sealing with a decreased scarring of the puncture site. Instead, during elevated temperature testing at 70°C and above, *none of the samples healed*. Typically a plug of material was ejected with the projectile. This left a circular hole in the sample that was observed to be larger when punctured at higher temperatures. However, there was a tendency toward healing as the materials were observed to minimize surface energy by

forming a smooth edged circular hole as shown in Figure 6-3. This result is in contrast to the wavy hole produced by non-healing LDPE as noted in Figure 4-2—there, wavy edges and a lack of elastic recovery were noted. Hence, contrary to expectations, increased temperature of film prior to puncture prevented the healing response.

Interestingly, for the 60°C test, two of the four materials showed possible healing—Nucrel® 925 and Surlyn® 8940. Here, the puncture site resembled RT tested samples, though the PBT has not been used to confirm healing. Given the 0% neutralization in the Nucrel® 925 and 30% in the Surlyn® 8940, ionic content can be ruled out as the reason for this also.

Though unexpected, the lack of self-healing during elevated temperature testing provided some ideas about the mechanics of the healing process. One very interesting result involving the temperature dependence of film response has been captured and compiled for easy visual comprehension as shown in Figure 6-4. A series of pictures illustrates a side view of punctured films which had been shot at different initial temperatures. It is determined that at room temperature, following initial stretching by the projectile, healing appeared to take place when the hole perimeter responded through a predominantly elastic mechanism in order to close the puncture. This behavior contrasted to the largely viscous or "flow" response of the perimeter at higher temperatures. This produced permanent deformation around the puncture site which dispersed the impact energy, preventing elastic recovery of the hole perimeter to close the puncture.

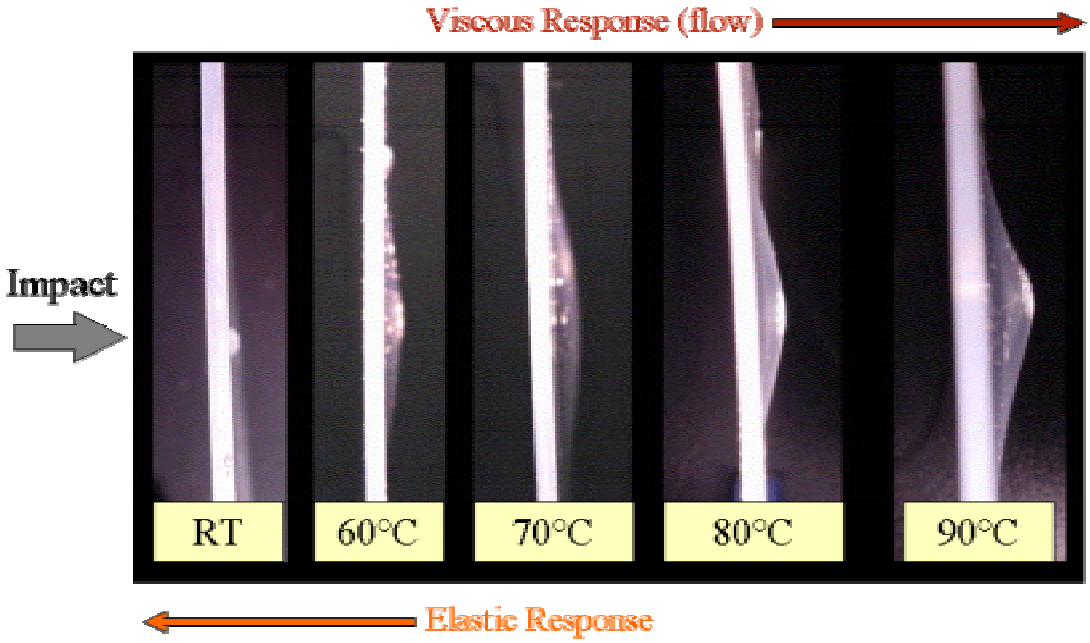

Figure 6-4 Viscoelastic response of the punctured films at various test temperatures. Rather than acting "stickier" at elevated temperatures, the heat energy already present in the system made the materials exhibit more plastic drawing (or in viscoelastic terms, a yielding response) and less elastic recovery allowing for more permanent drawing of the sample without the elastic recovery normally seen in the RT samples.

Though some samples may have healed at 60°C, overall no significant difference in the healing behavior was observed. To further support the room temperature data already discussed, ionic content showed no influence on the self-healing behavior. Further, a better understanding puncture/healing process was developed by examining samples tested over the full range of temperatures.

6.4.3 Quantitative Healing Data via Pressurized Burst Test

The pressurized burst test was used to examine samples shot at room temperature of all four materials. This produced a quantitative measure of the quality or "strength" of the healed puncture. Six samples of each material were examined. The results are given in Table 6-1 and plotted in Figure 6-5.

Table 6-1 Burst pressure of films of varying thickness following RT projectile testing.

Surlyn® 8940		Surlyn® 8920		Nucrel® 960		Nucrel® 925	
Thickness (mm)	Burst Pressure (psi)	Thickness (mm)	Burst Pressure (psi)	Thickness (mm)	Burst Pressure (psi)	Thickness (mm)	Burst Pressure (psi)
0.85	210	0.91	< 40	0.87	< 40	0.86	350
0.86	215	0.93	0	0.88	210	0.86	360
0.90	> 440	0.97	< 40	0.88	290	0.92	350
0.94	> 400	0.99	260	0.92	0	0.93	340
0.99	> 450	1.00	340	0.92	280	0.94	380
0.99	390	1.04	330	0.93	350	0.97	360

The quantitative results of Table 6-1 revealed some surprising differences. As described in Section 6.4.1, Nucrel® 960 and Surlyn® 8920 were the least reliable in their healing behavior with two and three failed samples respectively. Sample thickness did not appear to play a role in the failure of Nucrel® 960, though the failures in Surlyn® 8920 were of the three thinnest samples. This may indicate a stronger dependence on sample thickness for healing of Surlyn® 8920. This idea did not hold for Nucrel® 925 which healed over the range of thickness tested with very little difference in strength. It was easily the most consistent material tested with respect to these results having no failures and a comparatively high healed strength. Surlyn® 8940 also performed well by healing in every test. While its two thinnest samples burst on the low end of the scale, healing in three of the thicker films was too strong, not failing in the PBT. This may indicate a dependence of healing in Surlyn® 8940 on sample thickness also. Overall, Nucrel® 925 and Surlyn® 8940 performed the best during projectile testing by consistently healing with comparatively high strength.

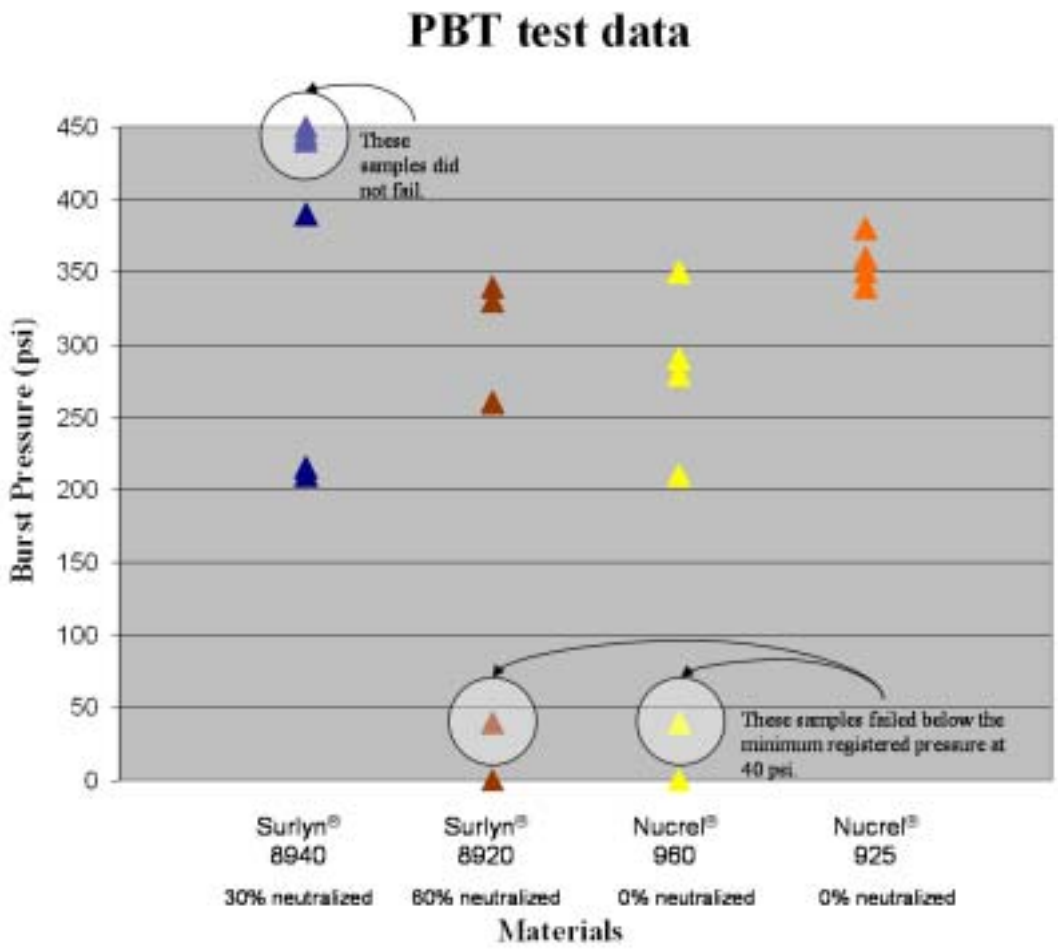

Figure 6-5 Burst pressure data from Table 7-1 is plotted for RT punctured samples of all four materials. It is noted that three samples of Surlyn® 8940 failed to burst during testing. Also, as noted in Section 6.4.1, some samples of Surlyn® 8920 and Nucrel® 960 failed below the minimum pressure recorded.

Thickness may have affected healing quality for the two Surlyn® samples though had no observed effect on Nucrel® 925 for the range tested. It is known that sample thickness will be involved in the maximum temperature reached by the films during puncture in a complex fashion, involving mass, energy transfer and elasticity. Sample thickness is also expected to affect the amount of material that remains following puncture in order to fill the void created. Thus, thickness is expected to have a significant effect on the healing process.

Quite unexpectedly, quantitative testing showed that ionic content is not only unnecessary for self-healing but that it does not produce better quality healing of the puncture sites. In fact, it may even inhibit healing in Surlyn® 8920 which contains the most ionic groups. Given the high pressures held by the healed films, the healing process is proved to contain a sealing component.

6.4.4 DSC

DSC data were nearly identical for the four EMAA materials tested post-puncture. First, an examination of samples located away from the puncture site showed the polymer had undergone an annealing process in the oven. This was determined by the appearance and shifting of an endothermic peak as shown in Figure 6-6 marked "Undamaged". *Tadano, et al,* suggested this annealing peak to be a "quasi-crystalline" peak rather than the order-disorder transition, T_i[10]. However, the possibility of this being T_i is not ruled out because the order-disorder peak has been observed to grow and shift with aging time (Section 3.4.2). It is known that during the annealing process, samples were heated above the T_i erasing the ordering of the ionic clusters. Rather than being cooled back to room temperature to begin reordering via the gradual aging process, they were held at these elevated temperatures. Though aging only ~5 minutes, it is hypothesized that during this time the ionic clusters began to reorder more quickly given the greater mobility at the increased annealing temperature. This phenomenon is common in semicrystalline polymers as crystallinity "ripens". Upon cooling, the order was locked-in, which subsequently produced the observed higher temperature annealing peak during the first DSC heat. The existence of this annealing peak in samples of Nucrel®, which would be expected to have no T_i, suggests the new annealing peak may be related to something other than ionic clustering. However, other studies have shown an order-disorder peak to exist in non-neutralized materials[1, 10]. Further investigation is ultimately necessary to determine the origin of this annealing peak.

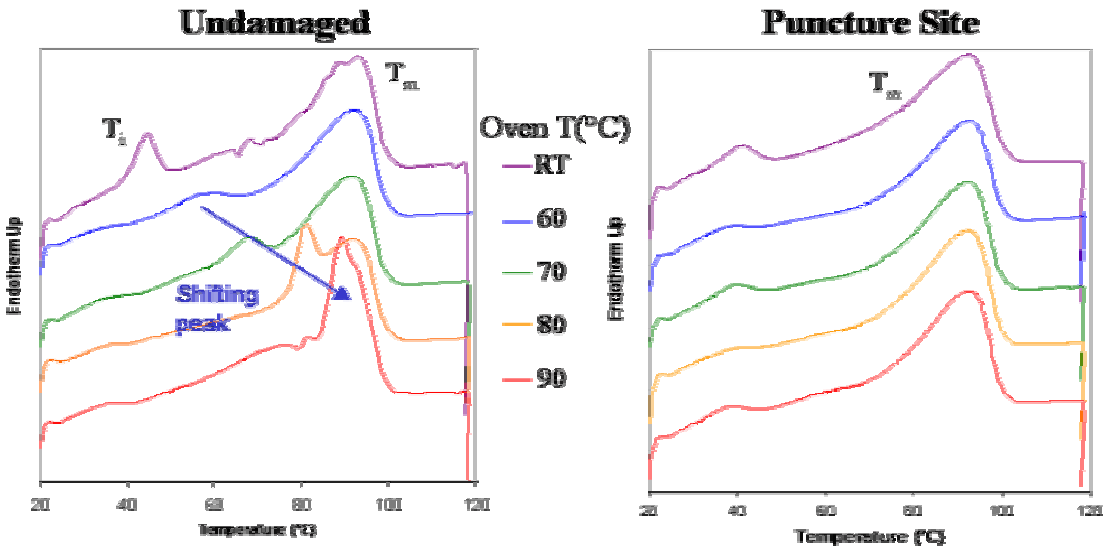

Figure 6-6 DSC first heat thermograms for Surlyn® 8940. All materials tested show a similar trend.

For material taken from the puncture site, DSC revealed that *the puncture/healing event erased the thermal history*. This was determined by a resetting of the T_i peak in Surlyn® samples, the disappearance of the shifted annealing peak for all materials, and identical curves for all puncture temperatures as shown in Figure 6-6 marked "Puncture Site". The erasure of thermal history confirms that samples heated to above the melt temperature locally during puncture-testing of this study as well (in addition to those by *Fall*[1]). Also, because there was no healing in the elevated temperature samples, it was determined that puncture (and the temperatures it produced) rather than healing erased the thermal history.

6.5 Conclusions

During room temperature testing, it was determined that samples of all ionomer and precursor materials expressed the self-healing behavior including even the non-neutralized base copolymers with only the acid groups present. This provided clear evidence that it is not strictly the ionic domains producing the self-healing behavior. Also, it was observed that already increased sample temperature hindered rather than helped the healing process. Instead, as shown in Figure 6-4, elevated temperature was

noted to help dissipate impact energy by promoting deformation of the sample, preventing the elastic response of the locally molten material to close the puncture. Quantitative measurements of the samples designated as “healed” during pressurized burst testing verified the existence of a sealing process. This quantitative data also proved that neutralization is not only unnecessary for quality self-healing in these particular copolymers, but that it may possibly hinder the healing response in Surlyn® 8920. The excellent performance of Surlyn® 8940 and Nucrel® 925 in the pressurized burst test and their possible healing at 60°C provides further evidence that the self-healing mechanism is independent of ionic content. More important may be the presence of the acid component in the copolymer which produces the synergy of mechanical properties necessary to make healing possible.

7. Design & Fabrication of Self-Healing CNT/Surlyn® composites

7.1 Introduction

The possibility of producing thermoplastic self-healing composites with enhanced mechanical properties using carbon nanotubes (CNT) is very attractive. Carbon nanotubes possess great potential as a reinforcing phase in composite materials. Examination of multi-walled carbon nanotubes (MWNT) has revealed extremely favorable mechanical properties including a Young's modulus on the order of ~0.8-1.3 TPa, tensile strength of ~150 GPa, and a bending strength of ~14 GPa[23-28]. Combined with a nanotube-polymer stress transfer efficiency an order of magnitude higher than current advanced composites[24], they hold much promise for use as a reinforcing material. One major problem, however, is their tendency to agglomerate under mixing conditions, leading to poor dispersion in composite materials[29, 30]. Hence, a number of techniques have been attempted in order to produce quality nanotube composite materials having well dispersed filler. These include solution casting of films[31-33], solution casting followed by pressing[34], *in situ* polymerization[35], and melt blending[29, 36, 37]. In addition, surfactants are sometimes employed to encourage dispersal of carbon nanotubes. Given the high solvent resistance of the ionomer resins in this study and their thermoplastic nature, a melt blending process was chosen for production of composite samples. A technique similar to that of *Jin, Z, et al* was used[29].

This chapter will investigate the fabrication and characterization of novel carbon nanotube filled Surlyn® composites. The materials produced were analyzed for mechanical property gains and their performance in self-healing was examined.

7.2 Materials

7.2.1 Matrix

Surlyn® 8940 resin was selected as the matrix material for composite samples. This EMAA ionomer was chosen for its excellent performance in projectile testing as presented above in this thesis and its moderate amount of neutralization.

7.2.2 Reinforcement

Multi-walled carbon nanotubes (MWNT) were chosen for the reinforcing phase of the composite. MWNT from Guangzhou Yorkpoint New Energy Sci. & Tech. Development Co., Ltd. (China) were selected. These MWNT were produced by chemical vapor deposition yielding a product of ~95% purity with nanotubes on the order of 10-40 nm in diameter. A representative TEM provided by the manufacturer is given Figure 7-1.

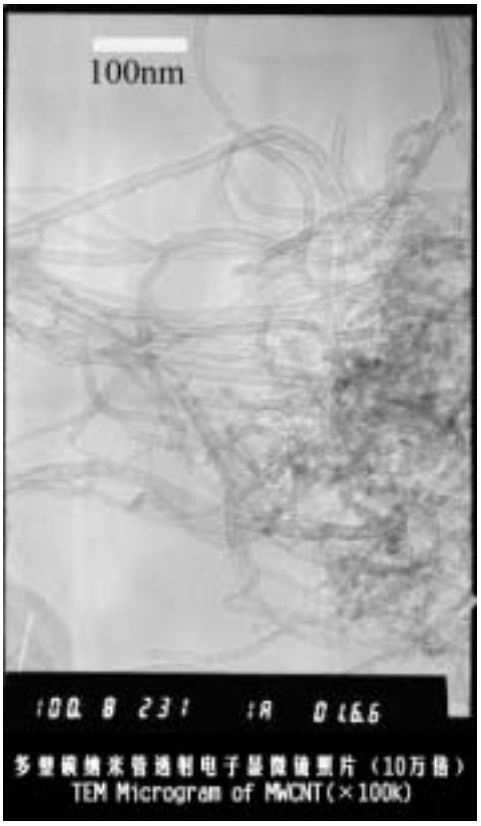

Figure 7-1 TEM of supplied multi-walled carbon nanotubes[38].

7.3 Fabrication

7.3.1 Composite

The composite consisted of Surlyn® 8940 containing 4 wt% MWNT. A dry mixture of pelletized resin with nanotubes was prepared by first weighing out specific amounts of each component. These materials were then combined in a jar and manually agitated in an attempt to premix/pre-disperse the materials prior to melt mixing. The dry mix was added to a preheated (180°C) C.W. Brabender® Plasti-Corder® with mixing bowl and mixed for 12 min at 80 rpm with roller-style mixing blades. After mixing, the molten blend was removed from the mixing bowl and placed in a mold between Teflon® release films. The material was allowed to reheat in the hot press at 190°C for 5 min. Gradually the platens were brought together allowing the sample to relax prior to application of 30,000 lbs for 90 s. Finally, samples were removed from the press and cooled on the lab bench. This produced a ~1.53 mm thickness opaque gray-black film. Samples were stored in a desiccator until testing.

7.3.2 Control

The control sample consisted of pure Surlyn® 8940. It was prepared in the same manner as the composite with the elimination of the dry mixing step used to premix the MWNT. This process produced a clear film of ~1.53 mm thickness. Samples were stored in a desiccator until testing.

7.4 Testing Procedures

7.4.1 Microscopic Characterization

In order to determine the extent of dispersion of the MWNT in the ionomer matrix, a sample of the composite material was freeze-fractured in liquid nitrogen and examined by

field emission scanning electron microscopy (FE-SEM) using a LEO 1550 Field Emission Electron Microscope. As the traditional SEM mode yielded very poor pictures, the InLens detector of the FE-SEM was used and produced much clearer images with greater contrast.

In addition to FE-SEM, an ISI SX40 scanning electron microscope was used to examine projectile-punctured samples. Samples were sputter-coated with gold and the puncture site was examined.

7.4.2 TGA

The TA Instruments Hi-Res TGA 2950 was used to perform thermogravimetric analysis (TGA) on produced samples. The specific method ramped temperature from RT to 800°C at 10°C/min in a nitrogen gas environment.

7.4.3 DSC

The same DSC setup as used in Section 3.3.3 was used. The specific procedure involved the following:

(1) Equilibrate at 20°C
(2) First Heat to 140°C at 5°C/min
(3) First Cool to 20°C at -10°C/min
(4) Second Heat to 140°C at 5°C/min

7.4.4 Mechanical Properties

Rectangular bars of approximately 1.3 x 6.35 cm were cut (thickness ~1.53 mm) and uniaxially deformed in an Instron® 5500R Model 1123 testing machine at a rate of 2 mm/min. These samples were allowed to extend past their yield point and plastically deform. Testing was conducted at room temperature.

7.4.5 Projectile Testing

Projectile tests followed procedures presented in Chapter 6. Testing was conducted at room temperature on films of approximately 1.53 mm in thickness.

7.5 Results

7.5.1 Microscopic Characterization

FE-SEM analysis of freeze-fractured composite samples revealed a uniform dispersion of MWNT in the ionomer matrix as shown in Figure 7-2. No large agglomerated regions were noted. Some smaller agglomerations are circled in this figure.

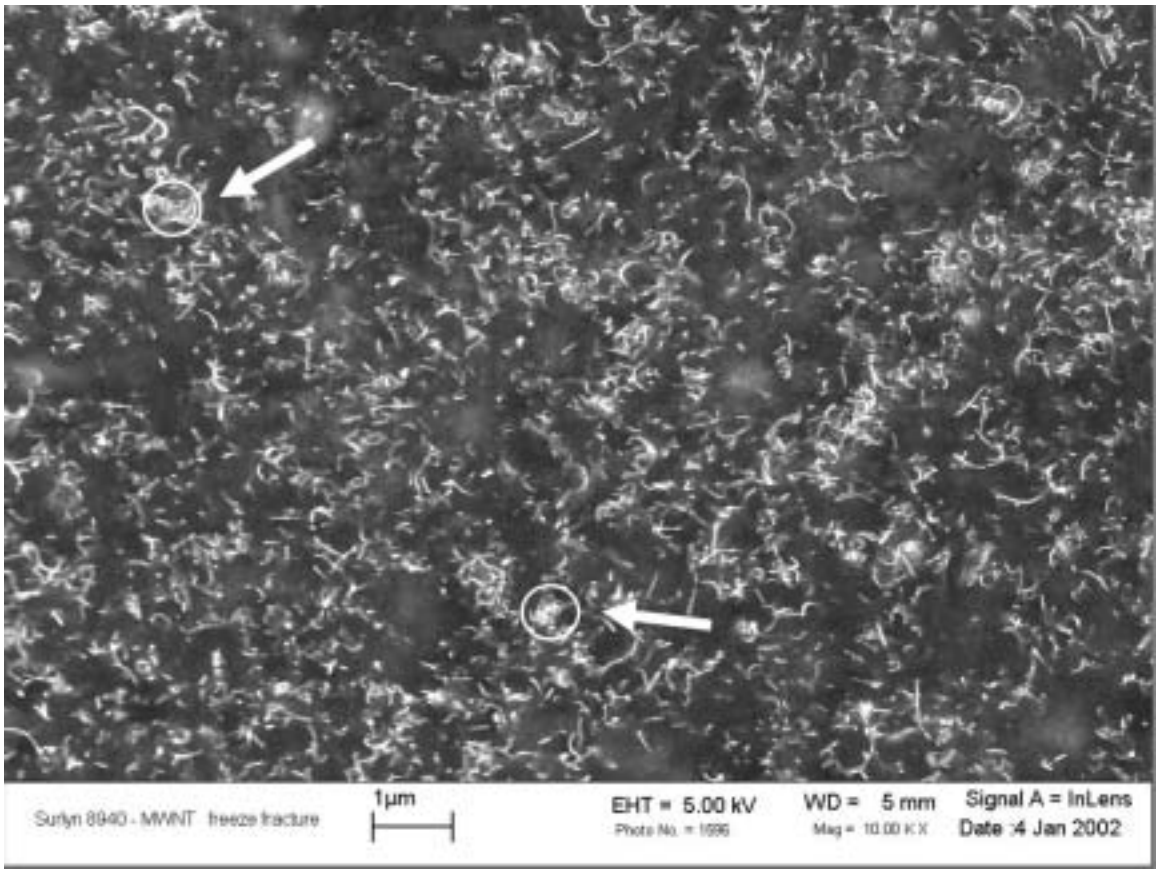

Figure 7-2 SEM micrograph of composite at 10kX magnification. Arrows indicate minor agglomerations which are circled.

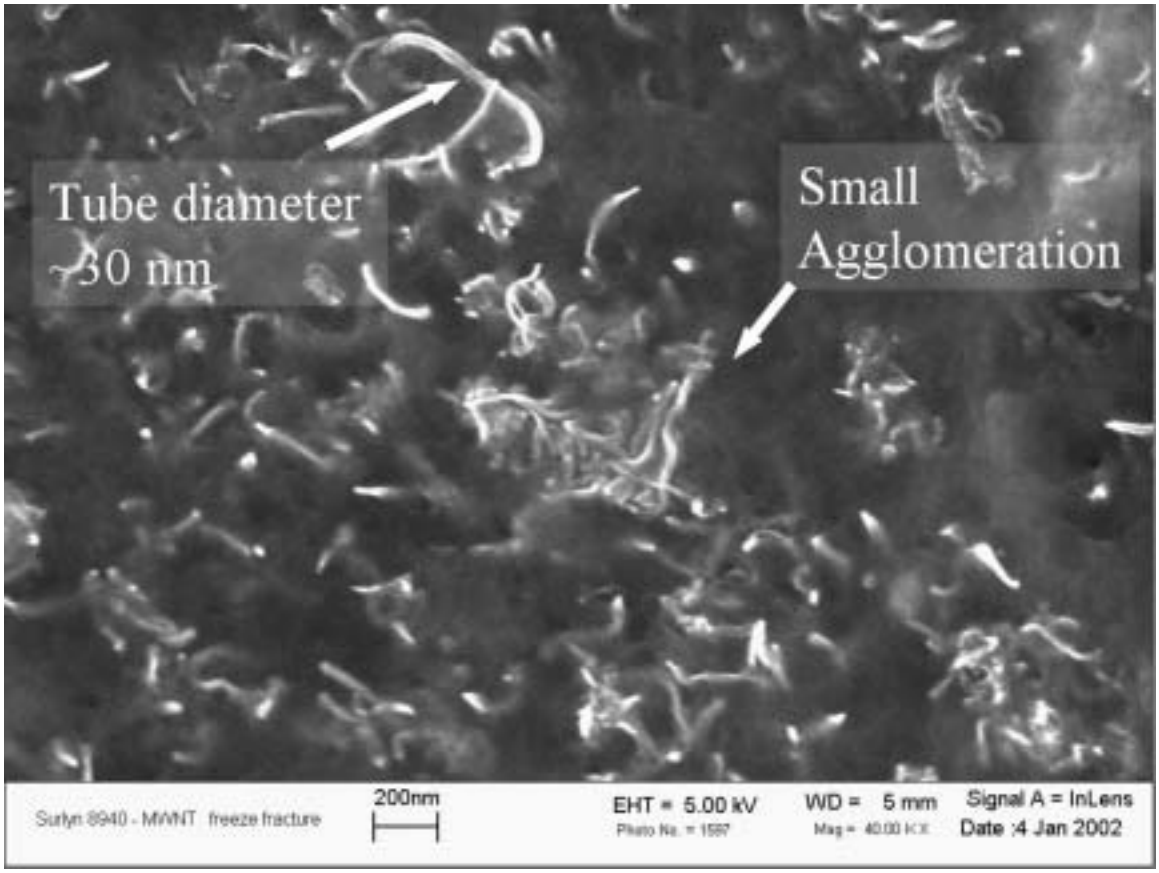

Figure 7-3 SEM micrograph of composite at 40kX magnification.

In Figure 7-3, FE-SEM verified the diameter of the MWNT to be in the range specified by the manufacturer. One of these minor agglomerated regions is noted though the ionomer appears well interspersed with the agglomerated tubes indicating good compatibility between the materials. Overall, microscopy revealed the melt mixing process was effective in dispersing MWNT in the ionomer matrix producing quality composite materials.

7.5.2 TGA

TGA revealed moisture content of the composite samples to be ~1 wt% vs. ~1.5 wt% for the control sample. As shown in Figure 7-4, the full TGA scan reveals the composite sample to be more thermally stable than the pure ionomer control specimen. The onset point of degradation is delayed from 400°C to 435°C. Thus the incorporation of MWNT

into the EMAA matrix provided a stabilizing effect, delaying polymer degradation. This is consistent with results of a *Jin, Z, et al*[29].

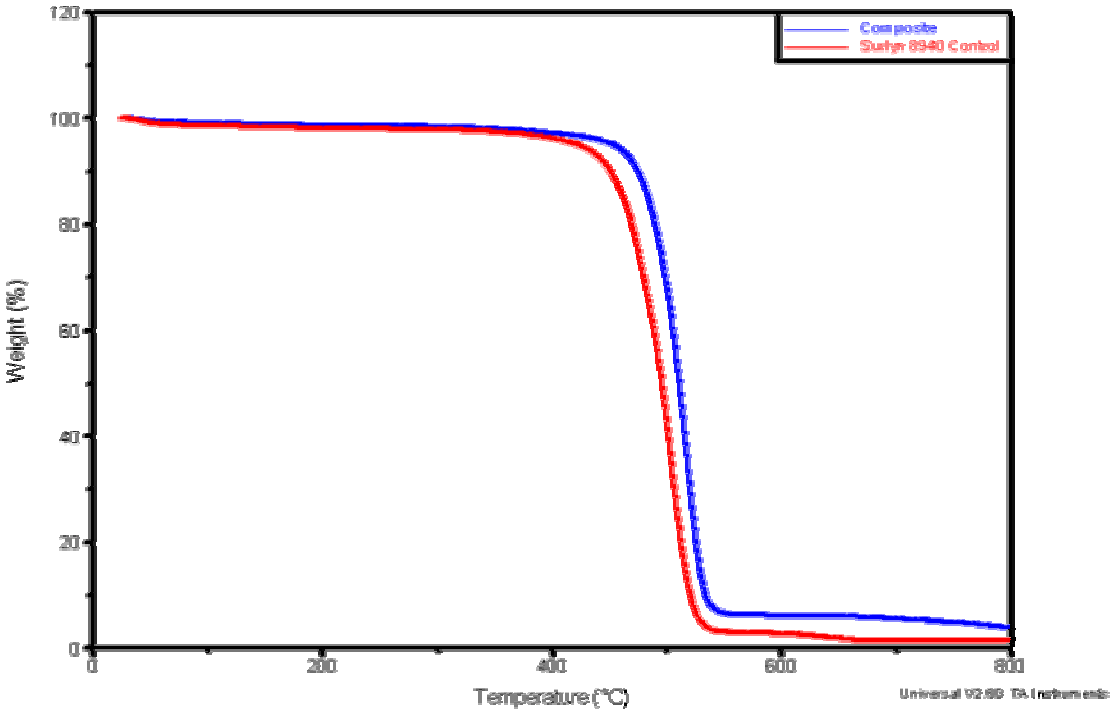

Figure 7-4 TGA of composite vs. Surlyn® 8940 control. Composite is more thermally stable.

7.5.3 DSC

DSC data revealed a difference in the crystallite formation of the composite versus the control sample. During the cooling step following the initial heat, analysis of the curves indicated a decrease of ~13% in crystallization compared to the control sample as shown in Figure 7-5. It is noted that this crystallinity loss typically acts to improve impact properties though its effect on healing is unknown.

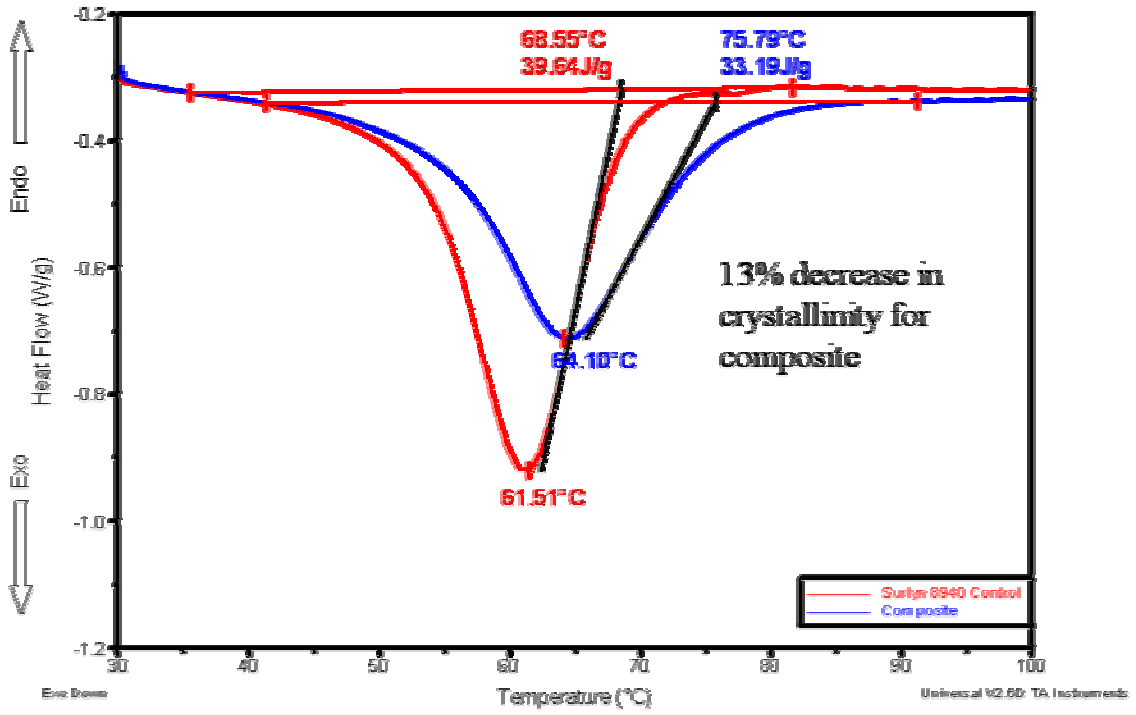

Figure 7-5 Crystalline formation during 10°C/min cooling step. Composite shows a 13% decrease in crystallinity vs. control sample.

The order-disorder peak was also examined. Samples of both composite and control were analyzed at ~5 months aging time and compared to initial runs at less than 1 day after fabrication. Analysis revealed ionic ordering was more developed for the composite material vs. the control as indicated by the increased enthalpy of the T_i peak shown in Figure 7-6. This composite T_i peak was also noted to be shifted to higher temperature indicating a faster "aging" process as discussed in previous chapters. By adjusting the obtained enthalpy value to account for the weight of the carbon nanotubes in the sample, a comparison was made for the enthalpy difference between the composite and control. This calculation determined a ~14% increase in the enthalpy of the composite T_i peak over the control. It was concluded that the hindrance of crystallite formation in the composite samples led directly to the increase in ionic ordering. Here, the lower crystalline content provided the polymer chains with greater mobility allowing a faster, less restricted ordering of the ionic clusters.

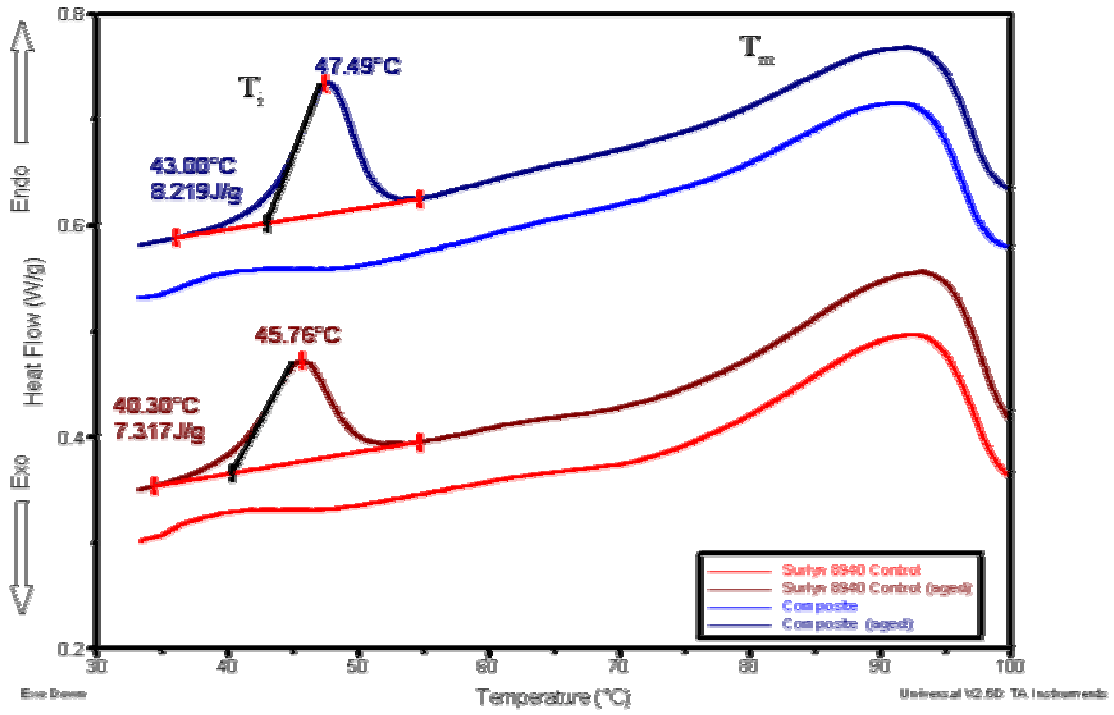

Figure 7-6 T_i transition of aged samples. Composite shows "faster" (more developed) aging of the ionic clusters.

7.5.4 Mechanical Properties

Testing revealed that substantial increases in key mechanical properties were produced by incorporation of the nanotubes. The addition of only 4 wt% nanotubes produced data as summarized below in Table 7-1. While poor quality samples should have a loss of mechanical integrity due to inadequate integration of filler material and poor fiber-matrix bonding, the observed mechanical gains indicate dispersion was effectively accomplished using the melt mixing technique.

Table 7-1 Table of composite properties.

	Surlyn® 8940 Control	*Composite*	*Increase*
Young's Modulus (MPa)	***2.19***	***2.64***	***21%***
Tensile Strength at Yield (MPa)	***15***	***17***	***13%***
Toughness at 5% strain (kJ/m^3)	***269.9***	***307.4***	***14%***

7.5.5 Projectile Testing

Projectile testing of the nanotube composites revealed quite promising results. Surprisingly, composite samples were observed to heal following projectile puncture at RT. This was initially verified using the liquid penetration test; however, given the deficiencies in this method discussed, another method was used. For better verification (prior to incorporation of the PBT described above), the post-puncture site was examined in detail via scanning electron microscopy. In Figure 7-7, both the entrance (front) and exit (back) sides of the healed region are shown (note: front and back are not matched to same sample). As seen in the image of the entrance side, the hole is observed to be tightly closed, indicating self-healing. However, much damaged material is noted on the exit side. To the naked eye, this exit side damage was much greater for the composite when compared to the neat polymer samples described above in other sections of this thesis. A definite loss in the some of the healing character was indicated, though a clearly healed puncture shown in the front-side image noted the healing ability was still maintained. As shown in the figure, the lighter shaded "rings" on the impact side provide possible evidence of the projectile diameter. When measured, the outer ring shown is actually ~1 mm smaller than the projectile diameter. This fact, in addition to the even smaller size of the remaining "crack", indicates a recoverable drawing without fracture of the localized perimeter of the film during puncture.

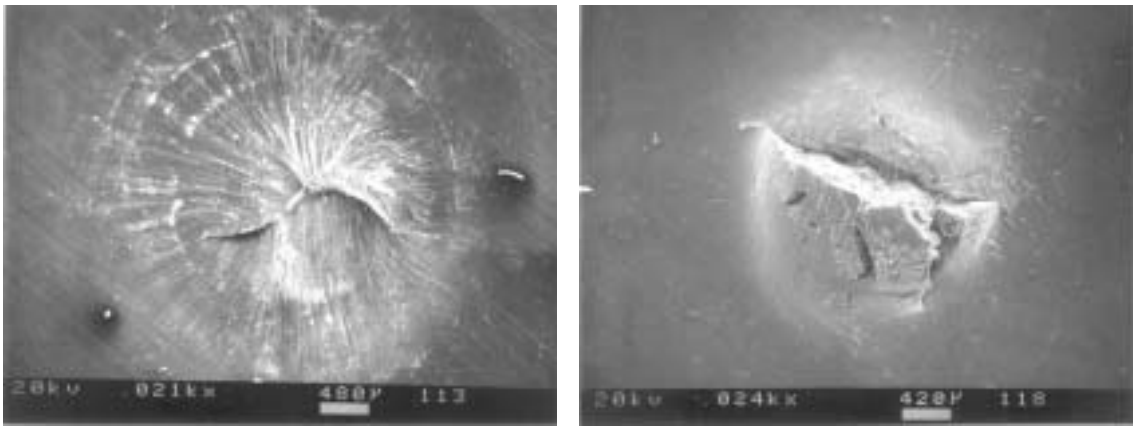

Figure 7-7 SEM micrographs of healed composite. Impact side (left) and exit side (right).

Closer examination of the healed area reveals much alignment of the material in the puncture direction as shown in Figure 7-8. No obvious separation of the healed material "flap" borders is noted.

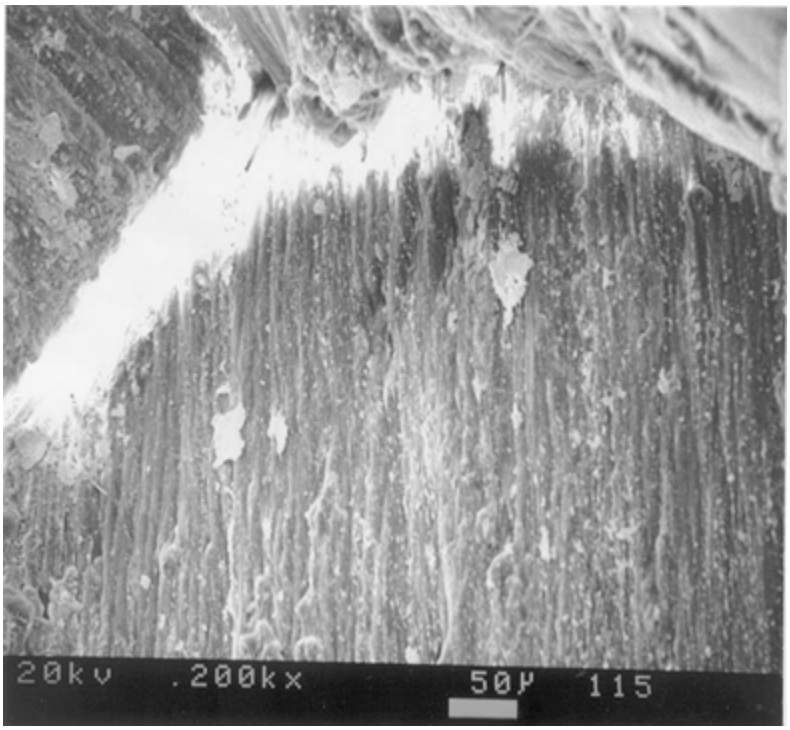

Figure 7-8 Magnified "flap" borders showing alignment of material on impact surface in direction of drawing during puncture.

7.6 Conclusions

Carbon nanotube filled ionomer composites were produced using a melt blending process. FE-SEM analysis and mechanical properties testing proved adequate dispersion can be obtained by melt mixing methods using a Brabender® mixer under the described conditions. TGA results showed that the MWNT added stability against the degrading effects of elevated temperatures. DSC indicated the MWNT caused a drop in crystallinity and that composite samples form the order-disorder peak—in fact, the peak was enhanced by the reduced crystalline content. Mechanical tests showed an augmentation of some bulk properties of these materials. Projectile testing provided further evidence of the self-healing behavior of ionomer materials in general. SEM of healed punctures revealed that these materials are able to stretch with impact, puncture, and then recover. Further testing is necessary to verify the strength of the healed hole as well as the healing ability of materials of varying amounts of filler. However, the above results show substantial potential for the development of tailored self-healing ionomer composites having enhanced performance.

8. Conclusions

The results of this study provided a clearer understanding of the mechanism of self-healing in EMAA materials. It was also proved that ionic neutralization of the copolymer is not necessary for the self-healing behavior expressed by these materials.

General observations of various damage infliction techniques showed high energy, high friction events such as sawing and projectile impacts to be favorable to healing. The most interesting and potentially useful example of self-healing was expressed during projectile penetration. As shown, in order to elicit healing, the puncture process must occur quickly without prolonged loading. Such a protracted event as shown for the nail puncture would act to hinder the elastic response of the healing process by producing permanent yielding in the polymer. Hence the need for a discrete impact loading/unloading event was determined. Multiple punctures of films, showed the healing behavior to be potentially reproducible.

Peel test experiments revealed that the increased temperature known to occur at the puncture site provided materials with greater mobility and increased interdiffusion ability. Though this did not lead to healing of preheated films (due again to permanent deformation which inhibited the elastic response necessary to healing), it was key in providing a quality sealing component as the final stage of healing. This was revealed by the high pressures held during pressurized burst testing of punctured films at room temperature. Projectile testing showed ionic content as unnecessary to self-healing, perhaps even hindering the healing response in some cases. Puncture tests also confirmed healing was produced by a local melt elastic response which closed the puncture.

With respect to the multi-wall carbon nanotube composites, the melt mixing method was shown to effectively produce quality composite materials with carbon nanotube filler well integrated into the EMAA matrix. By still expressing the self-healing response upon

projectile testing, great potential for producing custom self-healing composites is displayed. SEM analysis of the punctured materials also further uncovered the mechanics of the healing process.

In summary, a fuller understanding of the healing phenomenon has been revealed. Rather than by simple ionic attraction, healing is determined to be the product of a synergy of thermomechanical properties due to the addition of the methacrlyic acid component to the polyethylene structure. The self-healing behavior occurs upon projectile puncture whereby energy must be transferred to the material during impact both elastically (stored) and inelastically (dissipated as heat through friction). This process acts to heat the local puncture site to the melt state and is accompanied by an initial drawing of the local film. The film then fails allowing the projectile to pass through. Using the cooler, more rigid perimeter area around the puncture site as a frame, the polymer then responds with sufficient melt elasticity to rebound and close the hole. The molten surfaces finally bond together and interdiffuse in order to seal the hole on a very short time scale. The two main requirements expected necessary to produce the self-healing behavior are the need for the puncture event to produce a local melt state in the polymer material and for that molten material to have sufficient melt elasticity to snap back and close the hole.

9. Proposed Future Testing

A number of future test methods can further uncover the capabilities of the healing behavior and be used to examine the conclusions of this study.

One possible technique is the use of a high speed camera in order to observe the puncture/healing process. This would be expected to provide a better understanding of the dynamics of the healing event and verify the above conclusions.

Controlled projectile testing could be used to determine the capabilities and limitations of the self-healing process. An examination of various projectile speeds, sample thicknesses, and sub-ambient temperatures could reveal more about the unique self-healing behavior. Pressurized burst testing could test both the above films following healing and others including multi-punctured films to better understand re-healing abilities. Further, virgin or non-shot samples could be tested by the pressurized burst test in order to determine their pressure holding limitations. By comparing the pre- and post-shooting burst pressure, this would allow the “strength recovery” of healed samples to be determined providing an idea of how much damage the puncture event has done to these materials.

Finally, several other polymers can be tested in order to find other materials that exhibit this unique behavior.

10. References

1. Fall, R.A., *Puncture Reversal of Ethylene Ionomers--Mechanistic Studies*, in *Department of Chemistry*. 2001, Virginia Tech: Blacksburg, VA.
2. Tant, M.R. and G.L. Wilkes, *Viscoelastic Behavior of Ionomers in Bulk and Solution*, in *Structure and Properties of Ionomers*, A. Eisenberg, Editor. 1987, D. Reidel Publishing Co.: Dordrecht. p. 191-226.
3. Eisenberg, A. and M. Rinaudo, *Polyelectrolytes and Ionomers.* Polymer Bulletin, 1990. **24**(6): p. 671-671.
4. Eisenberg, A., *Clustering of Ions in Organic Polymers. A Theoretical Approach.* Macromolecules, 1970. **3**(2): p. 147-154.
5. Eisenberg, A., B. Hird, and R.B. Moore, *A New Multiplet-Cluster Model for the Morphology of Random Ionomers.* Macromolecules, 1990. **23**(18): p. 4098-4107.
6. Bellinger, M., J.A. Sauer, and M. Hara, *Tensile Fracture Properties of Sulfonated Polystyrene Ionomers .1. Effect of Ion Content.* Macromolecules, 1994. **27**(6): p. 1407-1412.
7. Statz, R., *Ethylene Copolymer Ionomers*, in *History of polyolefins : the world's most widely used polymers*, T. Cheng, Editor. 1986, D. Reidel: Dordrecht. p. 177-192.
8. Rees, R., *Ionomeric Thermoplastic Elastomers Early Research--Surlyn and Related Polymers*, in *Thermoplastic Elastomers: a Comprehensive Review*, H.E. Schroeder, Editor. 1987, Carl Hanser Verlag: Munich. p. 231-243.
9. Hara, M. and J.A. Sauer, *Mechanical Properties of Ionomers.* Journal of Macromolecular Science--Reviews in Macromolecular Chemistry and Physics, 1994. **34**(3): p. 325-373.
10. Tadano, K., E. Hirasawa, H. Yamamoto, and S. Yano, *Order-Disorder Transition of Ionic Clusters in Ionomers.* Macromolecules, 1989. **22**(1): p. 226-233.
11. Brust, G., *The Macrogalleria-Ionomers*, *http://www.psrc.usm.edu/macrog/ionomer.htm*, University of Southern Mississippi;1995-1996.
12. White, S.R., N.R. Sottos, P.H. Geubelle, J.S. Moore, M.R. Kessler, S.R. Sriram, E.N. Brown, and S. Viswanathan, *Autonomic healing of polymer composites.* Nature, 2001. **409**(6822): p. 794-797.
13. Yang, F. and R. Pitchumani, *Healing of thermoplastic polymers at an interface under nonisothermal conditions.* Macromolecules, 2002. **35**(8): p. 3213-3224.
14. Boiko, Y.M., G. Guerin, V.A. Marikhin, and R.E. Prud'homme, *Healing of interfaces of amorphous and semi-crystalline poly(ethylene terephthalate) in the vicinity of the glass transition temperature.* Polymer, 2001. **42**(21): p. 8695-8702.
15. Wool, R.P., *Polymer Interfaces: Structure and Strength*. 1995, Cincinnati: Hanser/Gardner Publications. 494.
16. Kutsumizu, S., N. Nagao, K. Tadano, H. Tachino, E. Hirasawa, and S. Yano, *Effects of Water Sorption on the Structure and Properties of Ethylene Ionomers.* Macromolecules, 1992. **25**(25): p. 6829-6835.

17. DuPont, *Surlyn Resin Molding Guide*, *http://www.dupont.com/industrial-polymers/surlyn/H-37063-2/H-37063-2.html*.
18. Kutsumizu, S., K. Tadano, Y. Matsuda, M. Goto, H. Tachino, H. Hara, E. Hirasawa, H. Tagawa, Y. Muroga, and S. Yano, *Investigation of microphase separation and thermal properties of noncrystalline ethylene ionomers. 2. IR, DSC, and dielectric characterization.* Macromolecules, 2000. **33**(24): p. 9044-9053.
19. Hirasawa, E., Y. Yamamoto, K. Tadano, and S. Yano, *Formation of Ionic Crystallites and Its Effect on the Modulus of Ethylene Ionomers.* Macromolecules, 1989. **22**(6): p. 2776-2780.
20. Russell, W.J. and E.A. Garnis, *A chromate-free low toxicity method of preparing aluminum surfaces for adhesive bonding.* SAMPE Journal, 1981: p. 19-23.
21. Lefebvre, D.R., B.K. Ahn, D.A. Dillard, and J.G. Dillard, *The effect of surface treatments on interfacial fatigue crack initiation in aluminum/epoxy bonds.* International Journal of Fracture, 2002. **114**(2): p. 191-202.
22. Rogers, N.L. *Pre-production evaluation of a nonchromated etchant for preparing aluminum alloys for adhesive bonding*. 1981.
23. Demczyk, B.G., Y.M. Wang, J. Cumings, M. Hetman, W. Han, A. Zettl, and R.O. Ritchie, *Direct mechanical measurement of the tensile strength and elastic modulus of multiwalled carbon nanotubes.* Materials Science and Engineering A-Structural Materials Properties Microstructure and Processing, 2002. **334**(1-2): p. 173-178.
24. Wagner, H.D., O. Lourie, Y. Feldman, and R. Tenne, *Stress-induced fragmentation of multiwall carbon nanotubes in a polymer matrix.* Applied Physics Letters, 1998. **72**(2): p. 188-190.
25. Wong, E.W., P.E. Sheehan, and C.M. Lieber, *Nanobeam mechanics: Elasticity, strength, and toughness of nanorods and nanotubes.* Science, 1997. **277**(5334): p. 1971-1975.
26. Salvetat, J.P., A.J. Kulik, J.M. Bonard, G.A.D. Briggs, T. Stockli, K. Metenier, S. Bonnamy, F. Beguin, N.A. Burnham, and L. Forro, *Elastic modulus of ordered and disordered multiwalled carbon nanotubes.* Advanced Materials, 1999. **11**(2): p. 161-165.
27. Salvetat, J.P., J.M. Bonard, N.H. Thomson, A.J. Kulik, L. Forro, W. Benoit, and L. Zuppiroli, *Mechanical properties of carbon nanotubes.* Applied Physics A-Materials Science & Processing, 1999. **69**(3): p. 255-260.
28. Lu, J.P., *Elastic properties of carbon nanotubes and nanoropes.* Physical Review Letters, 1997. **79**(7): p. 1297-1300.
29. Jin, Z., K.P. Pramoda, G. Xu, and S.H. Goh, *Dynamic mechanical behavior of melt-processed multi-walled carbon nanotube/poly(methyl methacrylate) composites.* Chemical Physics Letters, 2001. **337**(1-3): p. 43-47.
30. Park, C., Z. Ounaies, K.A. Watson, R.E. Crooks, J. Smith, S.E. Lowther, J.W. Connell, E.J. Siochi, J.S. Harrison, and T.L.S. Clair, *Dispersion of single wall carbon nanotubes by in situ polymerization under sonication.* Chemical Physics Letters, 2002. **364**(3-4): p. 303-308.

31. Jin, L., C. Bower, and O. Zhou, *Alignment of carbon nanotubes in a polymer matrix by mechanical stretching.* Applied Physics Letters, 1998. **73**(9): p. 1197-1199.
32. Shaffer, M.S.P. and A.H. Windle, *Fabrication and characterization of carbon nanotube/poly(vinyl alcohol) composites.* Advanced Materials, 1999. **11**(11): p. 937-941.
33. Stephan, C., T.P. Nguyen, M.L. de la Chapelle, S. Lefrant, C. Journet, and P. Bernier, *Characterization of singlewalled carbon nanotubes-PMMA composites.* Synthetic Metals, 2000. **108**(2): p. 139-149.
34. Muisener, P.A.O., L. Clayton, J. D'Angelo, J.P. Harmon, A.K. Sikder, A. Kumar, A.M. Cassell, and M. Meyyappan, *Effects of gamma radiation on poly(methyl methacrylate)/single-wall nanotube composites.* Journal of Materials Research, 2002. **17**(10): p. 2507-2513.
35. Jia, Z.J., Z.Y. Wang, C.L. Xu, J. Liang, B.Q. Wei, D.H. Wu, and S.W. Zhu, *Study on poly(methyl methacrylate)/carbon nanotube composites.* Materials Science and Engineering A-Structural Materials Properties Microstructure and Processing, 1999. **271**(1-2): p. 395-400.
36. Sennett, M., E. Welsh, J.B. Wright, W.Z. Li, J.G. Wen, and Z.F. Ren, *Dispersion and alignment of carbon nanotubes in polycarbonate.* Applied Physics A-Materials Science & Processing, 2003. **76**(1): p. 111-113.
37. Potschke, P., T.D. Fornes, and D.R. Paul, *Rheological behavior of multiwalled carbon nanotube/polycarbonate composites.* Polymer, 2002. **43**(11): p. 3247-3255.
38. GuangzhouYorkpoint, *TEM image of multi-walled carbon nanotubes,* *http://www.gzenergy.com/pic/c-cube.jpg*.

VITA

Stephen Kalista was born in Roanoke, Virginia on May 14, 1977 to Steve and Peggy Kalista. He spent the next 18 years of his life growing up in the picturesque valley town of Big Stone Gap in the mountains of Southwest Virginia. He graduated from Powell Valley High School in 1995 and entered Washington and Lee University in the fall of the same year. While at W&L he developed his love for the arts, languages, and sciences graduating *Magna Cum Laude* with a Bachelor of Science in Physics-Engineering in June of 1999. He then entered Virginia Tech in the fall of that year and following completion of this thesis will continue at Tech in pursuit of a Ph.D. in the Macromolecular Science and Engineering program. He has a love for cooking because he loves to eat good food especially Mexican, and he soon plans on getting a dog. One day he will be a college professor, with a focus on interdisciplinary teaching and providing undergraduate students with unique research opportunities.